(NASA-TM-X-73125) BASALT MODELS FOR THE MARS PENETRATOR MISSION: GEOLOGY OF THE AMBOY LAVA FIELD, CALIFORNIA (NASA) 56 p HC $4.50 CSCL 08G

N76-30619

Unclas
G3/42 49607

NASA TECHNICAL MEMORANDUM

NASA TM X-73,125

NASA TM X- 73,125

BASALT MODELS FOR THE MARS PENETRATOR MISSION: GEOLOGY OF THE AMBOY LAVA FIELD, CALIFORNIA

Ronald Greeley* and T. E. Bunch

*University of Santa Clara
Santa Clara, California 95053
and
Ames Research Center
Moffett Field, California 94035

April 1976

1. Report No. NASA TM X-73,125	2. Government Accession No.	3. Recipient's Catalog No.
4. Title and Subtitle BASALT MODELS FOR THE MARS PENETRATOR MISSION: GEOLOGY OF THE AMBOY LAVA FIELD, CALIFORNIA		5. Report Date 6. Performing Organization Code
7. Author(s) Ronald Greeley* and T. E. Bunch		8. Performing Organization Report No. A-6554
9. Performing Organization Name and Address *University of Santa Clara, Santa Clara, Calif. 95053 and Ames Research Center, Moffett Field, Calif. 94035		10. Work Unit No 195-21-04 11. Contract or Grant No.
12. Sponsoring Agency Name and Address National Aeronautics and Space Administration Washington, D.C.,20546		13. Type of Report and Period Covered Technical Memorandum 14. Sponsoring Agency Code
15. Supplementary Notes		

16. Abstract

Amboy lava field (San Bernardino County, California) is a Holocene basalt flow selected as a test site for potential Mars Penetrators. This report discusses 1) the general relations of basalt flow features and textures to styles of eruptions on Earth, 2) the types of basalt flows likely to be encountered on Mars and the rationale for selection of the Amboy lava field as a test site, 3) the general geology of the Amboy lava field, and 4) detailed descriptions of the target sites at Amboy lava field.

17. Key Words (Suggested by Author(s))		18. Distribution Statement	
Mars Penetrator mission Basalt flows Volcanism		Unlimited STAR Category — 42	
19. Security Classif. (of this report) Unclassified	20. Security Classif. (of this page) Unclassified	21. No. of Pages 56	22. Price* $4.25

*For sale by the National Technical Information Service, Springfield, Virginia 22161

TABLE OF CONTENTS

BASALT MODELS FOR MARS PENETRATOR MISSIONS:

GEOLOGY OF THE AMBOY LAVA FIELD, CALIFORNIA

Ronald Greeley
University of Santa Clara

and

Theodore Bunch
Ames Research Center

SUMMARY

Amboy lava field (San Bernardino County, California) is a Holocene basalt flow selected as a test site for potential Mars Penetrators. This report discusses 1) the general relations of basalt flow features and textures to styles of eruptions on Earth, 2) the types of basalt flows likely to be encountered on Mars and the rationale for selection of the Amboy lava field as a test site, 3) the general geology of the Amboy lava field, and 4) detailed descriptions of the target sites at Amboy lava field.

1.0 INTRODUCTION

Studies are currently in progress to determine the feasibility of penetrators as potential hard landers for a mission to Mars in the post-Viking period. Preliminary studies (Quaide, 1974); Briggs *et al.*, 1975; Cutts, 1975) show that an array of instruments could be placed on the martian surface via penetrators that would significantly advance knowledge of Mars. Although some tests have been conducted to determine the success of penetration in different materials, additional tests are required to determine the behavior of penetrators in geological settings appropriate for the full range of potential Martian sites.

A cooperative program of U. S. Geological Survey and university geologists sponsored by the Office of Planetology to map the geology of Mars was completed in 1975. Thirty geological quadrangles at a scale of 1:5,000,000 were completed which are currently being used to derive "best estimates" of terrains and surfaces most likely to be encountered on Mars. Although precise rock types[1] have not been defined on Mars, mapping results indicate that *at least* three general types of geological materials should be considered as potential penetrator sites: 1) eolian (wind) deposits, 2) basaltic lava flows, and 3) impact-generated regolith. Penetrator tests in eolian sediments

[1]The term *rock* refers to materials ranging from loose sediment to solid crystalline masses.

were conducted at McCook County, Nebraska, in early 1976 and the results are currently being analyzed. The next test is scheduled to be in a basaltic lava flow and, after the examination of several areas as potential sites (Bunch *et al.*, 1976), the Amboy lava field (figs. 1 and 2) was selected. Although there are many basalt flows in the western United States that might be suitable, Amboy was selected for three reasons: 1) previous NASA-sponsored studies (Watkins, 1965, 1966a,b) provide limited engineering data; 2) one of us (RG) has a project[2] in progress at Amboy, although it is not related to penetrators; and 3) the Amboy lava field conforms best to the evolution criteria for penetrator basalt sites (Bunch *et al.*, 1976).

This report discusses textures and terrain-types of terrestrial basalt flows, possible types of basalt flows on Mars, and the geology of the Amboy lava field, San Bernardino County, California, and its suitability as the test site. The data presented in this report are from previous studies and from field work conducted in 1976.

2.0 BASALT FLOWS ON EARTH

In order to understand the kinds of basalt surfaces likely to be encountered on Mars and to place the rationale of the Amboy test site in proper perspective, it is instructive to review some of the different types of basalt flows, their textures, and the kinds of terrains that result from eruptions of basaltic lava.

2.1 Basalt Flow Textures

The types of surfaces and textures that develop on basaltic lava flows are functions of many complex variables. Of primary importance are: 1) composition of the lavas, 2) temperature of extrusion and heat loss during flow, 3) flow viscosity (which itself is a function of many interrelated parameters), and 4) the content and nature of volatiles within the lava. A simple classification (Wentworth and Macdonald, 1953) recognizes three textures of basalt flows: pahoehoe, aa, and block lavas. Pahoehoe (fig. 3) is characterized by smooth, billowy textures and is representative of very fluid flows. Aa is characterized by a rough, jagged, clinkery surface (figs. 4 and 5), representing intermediate flow viscosities. Block lavas are typically composed of blocks of relatively massive lava up to a meter or more in diameter and are the result of highly viscous flows (fig. 6). It is not unusual for these three types to be transitional from pahoehoe to aa to block lavas, all within a single flow unit as the viscosity increases in the flow away from the vent. In some cases, pahoehoe can change directly to block lava without going through an intermediate aa stage; however, transition does not

[2]"Eolian Processes and Volcanic Landforms of Amboy Crater," sponsored by the Planetary Geology Program Office, NASA.

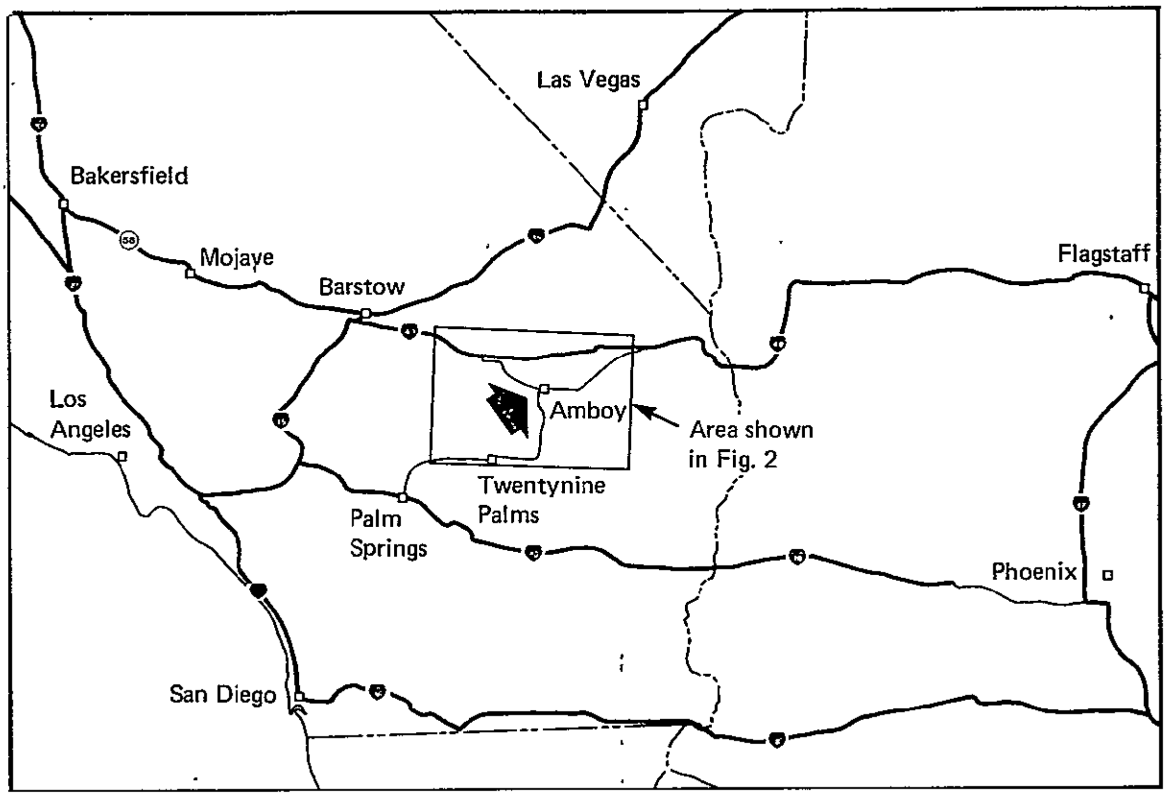

Figure 1.- Location of Amboy, San Bernardino County, California. Nearest regularly scheduled air service is in Palm Springs.

work in reverse, that is, block lava and aa cannot revert to pahoehoe. It is important to note that these three textures are primarily distinctive only for the surface of lava flows. At depths ranging from a few centimeters to a few meters, lava flows are typically massive, and if viewed only in cross section, it would be difficult or impossible to distinguish one lava type from another. In terms of total volume and surface area covered, pahoehoe lavas are by far the most extensive on Earth. Studies of the Moon, Mars, and Mercury indicate a similar pattern for those planets as well: Hence, most of this discussion is focused on pahoehoe textures.

Examination of the upper part of a typical fresh pahoehoe lava flow reveals that it can be subdivided into four intergradational zones: 1) an uppermost glassy crust, or rind, up to a few millimeters thick, 2) a frothy layer, consisting of glassy, finely vesicular lava up to a few centimeters thick, 3) a vesicular zone, consisting of crystalline and glassy basalt that is coarsely vesicular, and 4) a massive layer typically less vesicular than the upper zones and which may be tens of centimeters to tens of meters thick. Elston *et al.* (1976) in a study of basalt lava flows in New Mexico have demonstrated that after about two and one-half million years of erosion only the massive zone of most basalt flows remain (fig. 7). Although little is known about the weathering regime on Mars, active surface erosion is known

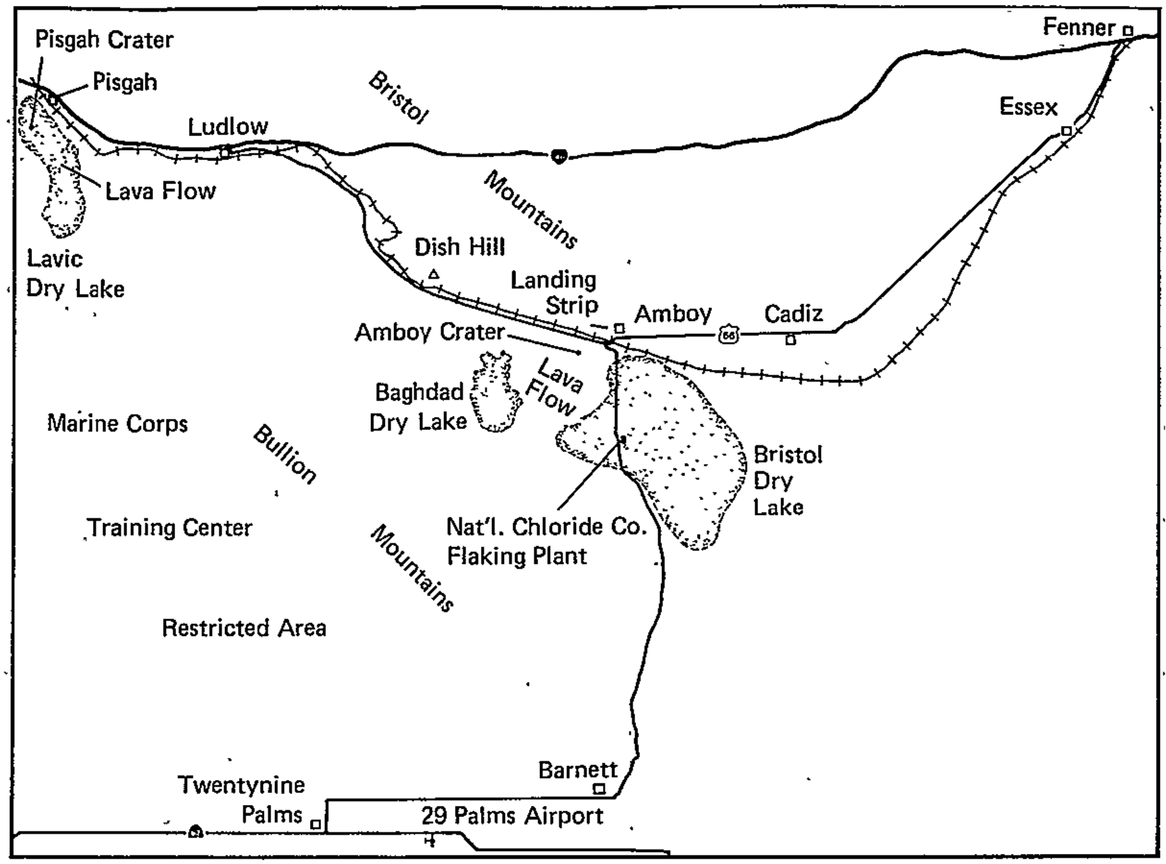

Figure 2.- Detail of the Amboy area, San Bernardino County, California.

to occur and it seems likely that most of the basalt flows on Mars would have the upper vesicular layers eroded away, with only the massive layers remaining.

The above discussion applies to "typical" pahoehoe flows. Closer examination of pahoehoe lava flows, however, shows that there are wide variations of surface textures and structures that will affect the penetrability. A recent study of active pahoehoe flows in Hawaii (Swanson, 1973) showed that there are at least three laterally gradational types of pahoehoe: 1) a cavernous type, termed shelly pahoehoe, characterized by fragile gas cavities, small lava tubes, and buckled fragments of crust; 2) "fountain-fed" pahoehoe — a comparatively smooth-surfaced, dense type that is characterized by small surface channels and few large cavities; and 3) "degassed" pahoehoe, a relatively dense type characterized by hummocky surfaces with abundant low tumuli and overlapping pahoehoe toes and lobes. Although "degassed" pahoehoe is often fed by lava tubes, it also can advance by budding pahoehoe "toes" which coalesce and accumulate as a massive flow front. These three types of pahoehoe are gradational and can be related qualitatively to the relative gas content and flowage for the lava. The variation in surface vesicularity of these flows, however, can be variable even within a singular

Figure 3.- Active lava lake at the summit of Mauna Ulu, Hawaii, and the formation of pahoehoe lava. Rapid cooling of the skin of the freshly erupted lava produces a glistening rind of glass on the pahoehoe. Photograph by Dale Cruikshank, University of Hawaii.

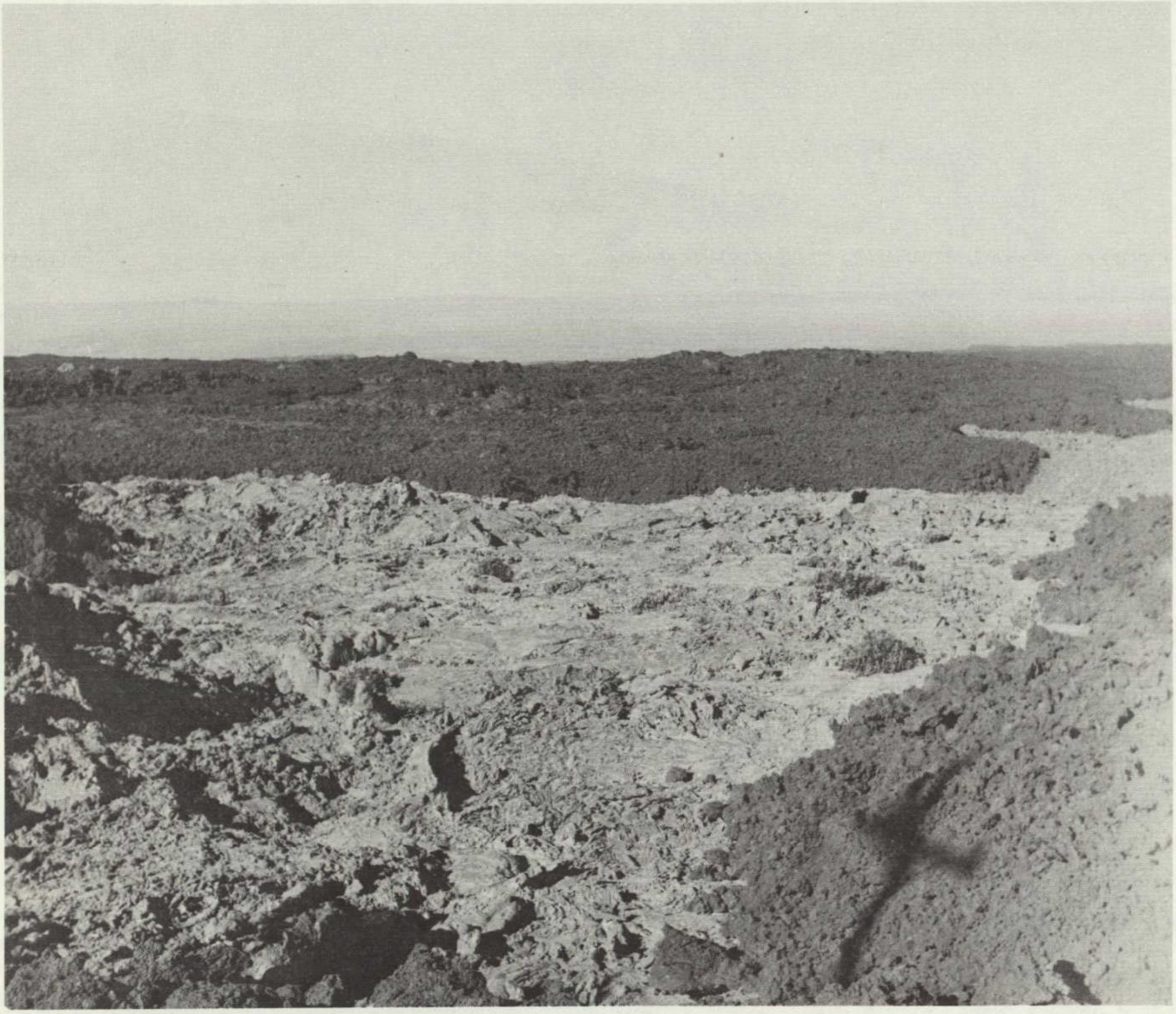

Figure 4.- Aa flows showing typical clinkery and rubbly surface texture (Humuula Saddle area, Hawaii). Photograph by Dale Cruikshank, University of Hawaii.

flow type. For example, table 1 (after Swanson, 1973) shows increasing viscosities and densities measured for an active lava flow, as related to distance from the vent.

From terrestrial analogies, we should expect highly vesicular and cavernous forms of basalt to be restricted to near-vent areas, and hence to be relatively rare on planetary surfaces, while "degassed" forms should be more common, particularly those that are "tube-fed." Even "degassed" forms, however, may be vesicular, especially toward the tops of flows. Of the candidate penetrator basalt test sites that have been examined, most of the sites involve lavas that are near vents and hence their vesicularity may not be representative of the basaltic plains and massive shield of large areal extent likely to be encountered on Mars.

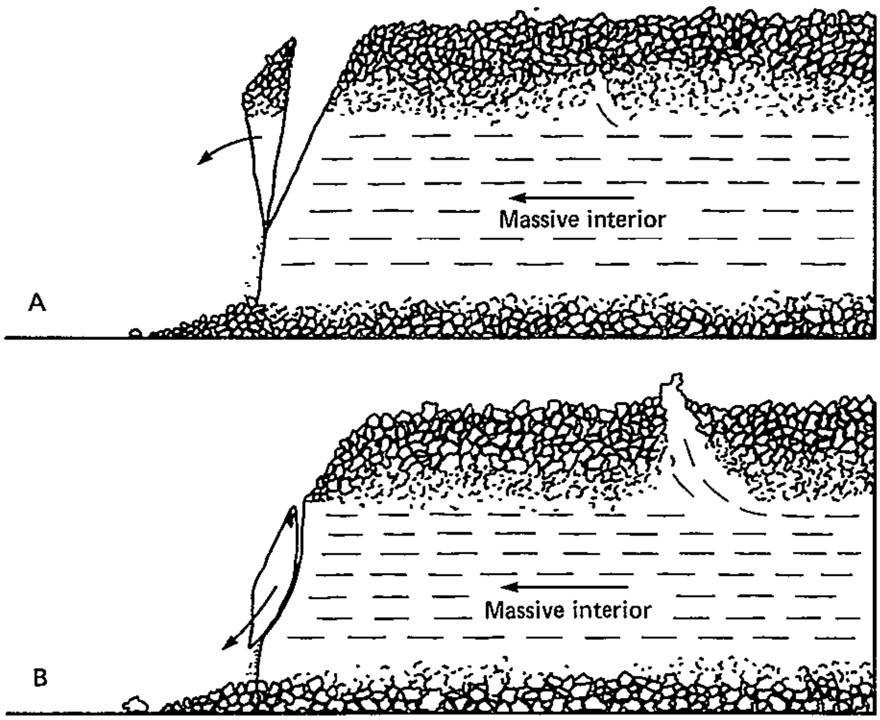

Figure 5.- Diagrams of advancing aa flow fronts, showing (A) a block tilting forward away from a crack separating it from the massive center of the flow; and (B) a block sliding downward and forward on a separation plane. Showers of incandescent sand are coming from the lower edge of the separating block. The arrows show the directions of flow movement and movement of the blocks. (After Macdonald, 1972.)

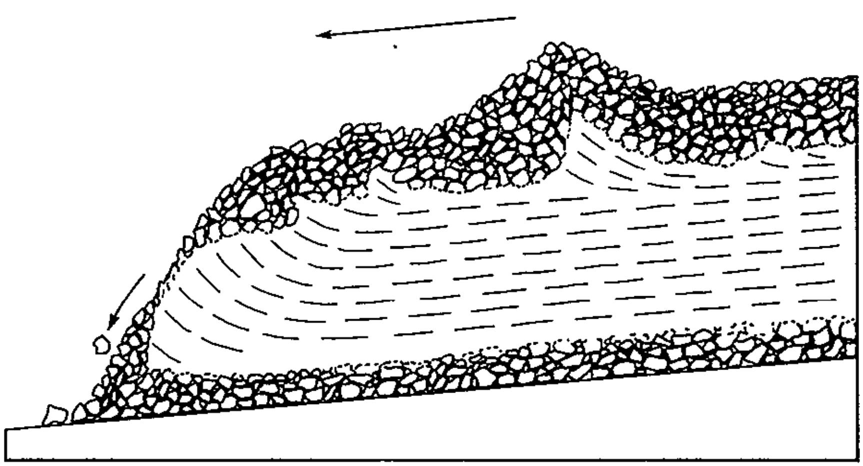

Figure 6.- Diagrammatic cross section of the front of a block lava flow showing platy jointing. The arrow indicates the direction of movement of the flow. Blocks on the bottom of the flow result from autobrecciation of the flow, and from the accumulation of blocks at the flow front that are overrun by the flow, like a tractor-tread. Blocky zone may be several meters or more thick and consists of blocks typically up to 1 m in diameter (after Macdonald, 1972).

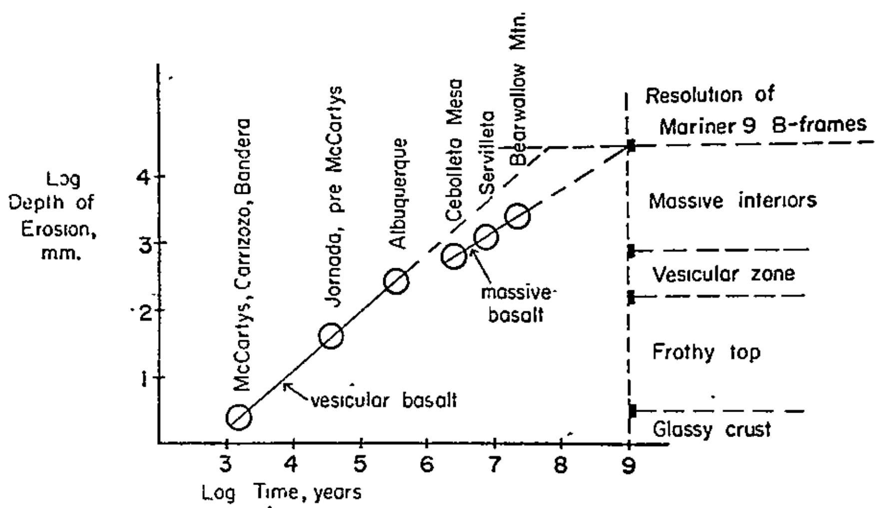

Figure 7.- Erosion rates of basalt flows, New Mexico (from Elston *et al.*, 1976).

TABLE 1.- SPECIFIC GRAVITIES OF TUBE-FED MOLTEN LAVA SAMPLES

(after Swanson, 1973)

Sample	Distance from vent (km)	Specific gravity	Vesicularity %	Comment
1	0	<1 to 1.49	50 to 70	Dipped from summit fissure
2	4.5	1.73	42	Collected through window in tube
3	10	1.84	38	Surface ooze fed by tube
4	12	2.48	18	Collected where lava emerges from tube at coastline

2.2 Basalt Terrain Types

On Earth the eruption of basaltic lavas can lead to the formation of many diverse terrains and geological provinces, shown in table 2. Landforms produced by eruptions of basalt are the result of complex, interrelated variables, the most important of which are: 1) rate of extrusion, 2) viscosity (a function of composition, volatile content, temperature, etc.), 3) preflow topography, and 4) nature of the vent(s) (central, fissure, etc.). Of the various types of basaltic terrains, three (fig. 8) appear to be the most important for interpreting large volcanic regions of the terrestrial planets (Greeley, 1976) — flood basalts, shield volcanoes and basaltic plains. *Flood basalts,* typified by the Columbia River Plateau, are erupted at rather high rates of effusion from linear vent systems (fissures) that may be more than 100 km long. Intervals between eruptions are comparatively long and subsequent eruptions seldom use the same fissure more than once. The resulting lava flows are massive and appear to have been ponded in vast lava lakes. Surface features such as lava flow channels and lava tubes are typically lacking, either because they did not form, or because they were destroyed by lava lake activity. Vent structures such as cinder cones and spatter cones are either absent or poorly developed. The rate of eruption on an hourly or daily basis appears to have been extremely high, producing great floods of lava which cooled as single flow units that may be 30 m or more thick.

Volcanic shields are also produced by relatively high rates of eruption, but the volumes of lava on an hourly or daily basis typically appear to be lower than those for flood basalts. Moreover, the vents are frequently point

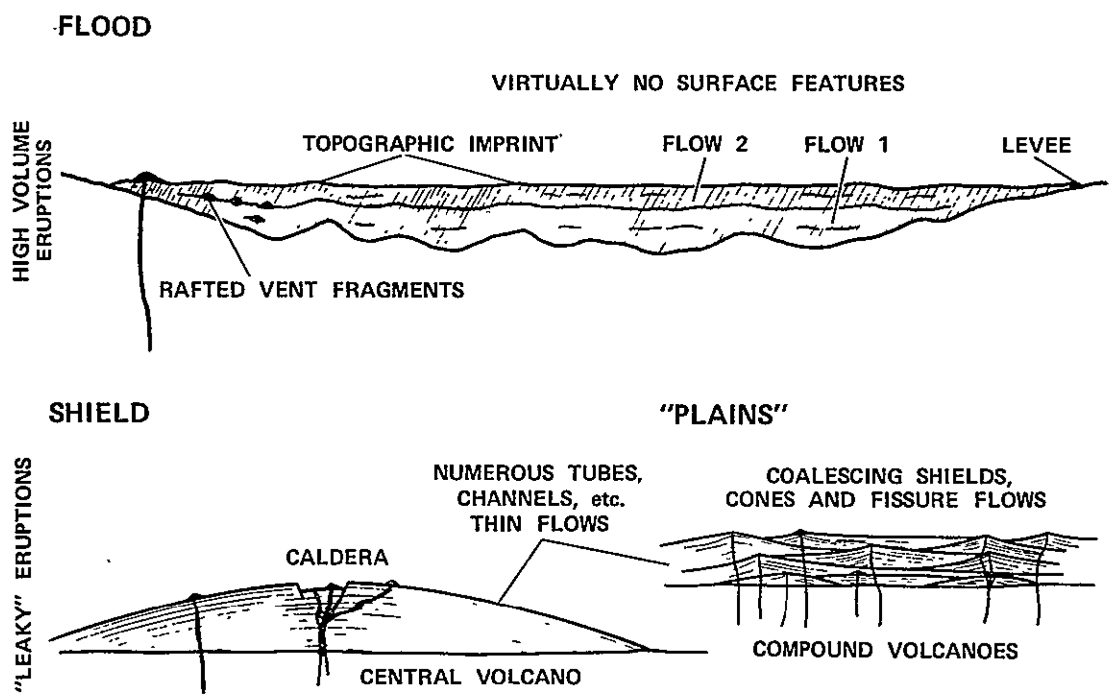

Figure 8.- Diagram of major basaltic landforms (after Greeley, 1976).

TABLE 2.- BASALTIC VOLCANOES

(after Greeley, 1976)

	Volcanic landform	Eruptive style	Typical lava texture	Comments
1.	Flood basalt plateau	Fissure eruption, high volume-highly fluid; few flow features	Pahoehoe Massive, dense, low vesicu-larity; vertical jointing	Common on planetary surfaces (1)
2.	Basalt "plains"	Fissure and central vent, moderately high volume and rate; fluid lavas; lava tubes and channels	Pahoehoe, tube and toe-fed; aa, variable, from massive to vesicular; vertical plating and joints	Common on planetary surfaces (2)
3.	Basaltic ash plains	Explosive	Pumiceous	Rare
4.	Shield volcanoes	Central vent with associated fissures; high rate, moderate volume, fluid lavas, lava tubes and channels	Pahoehoe, tube and toe-fed, vesicular, platy jointing	Common on planetary surfaces (2)
5.	Composite cones	Central vent, explosive alternating with flows, tubes and channels infrequent	Pyroclastics; vesicular to dense flows; pahoehoe and aa	Commonly associated with plate subduction zones (3)
6.	Cinder cones	Explosive, infrequent flows	Pyroclastics	Common on planetary surfaces (2)
7.	Domes	Central vent, low volume, low rate, viscous lavas	Block flows	Rare

(1) Earth, Moon, Mars, Mercury; (2) Earth, Moon, Mars; (3) Earth, Mars (?)

sources, rather than long fissures. Thus, the nature of the eruption is markedly different. For example, the eruptions at Mauna Ulu in Hawaii were essentially continuous over a period of five years, producing thin, tube-fed flows. Average flow thicknesses for Mauna Loa, the classic shield volcano on Earth is about 5 m, in contrast to the 30- to 40-m thickness flows in the Columbia River Plateau. Rapid outbursts of relatively short duration also occur on shield volcanoes, however, as evidenced by the 1975 summit eruption of Mauna Loa. Lava tubes and channels play an important role in the construction of shield volcanoes; a recent analysis of Mauna Loa (Greeley *et al.*, in preparation) shows that at least 80% of the flows exposed on the surface involved emplacement by lava tubes and channels.

Basaltic plains combine some of the characteristics of both flood basalts and shield volcanoes and is typified by the Snake River Plain in Idaho. This extensive region (Greeley and King, 1975) is made up of lava flows about 10 m thick that erupted from both point sources to produce small coalescing lava shields and short fissures that formed thin sheet flows. The combined thickness of all flows exceeds 2000 m in some places and in many respects, the Snake River Plain appears to resemble some of the smaller lunar maria. As in shield volcanoes, flow features such as lava tubes and lava flow channels are relatively common on basaltic plains.

Thus, it is possible to interpret the styles of eruption and modes of emplacement of basalt flows by the identification of surface features. Shield volcanoes are easily identified by their massive constructional character, central vents, and flow features such as lava tubes and channels. Flood basalts can be identified by their essentially featureless plateau-like surfaces that lack flow structures, while basaltic plains are identified by relatively flat surfaces containing lava tubes, lava channels, and rift zones.

3.0 STYLES OF VOLCANISM ON MARS

One of the major discoveries of the Mariner 9 mission to Mars was the existence of extensive volcanic features. Although initial analysis of Mariner 9 data led many investigators to believe that volcanism was relatively late in the evolution of the planet, subsequent studies have found highly degraded (hence, old) volcanic features in several areas, indicating that volcanism has extended over long periods in the history of the planet (Carr, 1973, 1974).

The geomorphology of the identified martian volcanic features indicates a basaltic composition, an interpretation substantiated by Earth-based spectroscopic observations. Silicic volcanics (rhyolites, ash flows, etc.) have not been positively identified, although some dome-shaped volcanic constructs (e.g., Tharsis Tholus) probably represent more viscous lavas which may be more silicic than basalt.

Of the possible types of basaltic terrains (table 2), three are known to cover extensive areas on Mars (fig. 9): 1) shield volcanoes (fig. 10), 2) lava plains (fig. 11), and 3) flood-basalts, all of which are important scientifically and, therefore, are potential Mars penetrator sites. As discussed above, it is unlikely that the glassy rind or the frothy zone would be preserved on most martian basalt flows. Moreover, on the martian flood and plains basalts (which make up most of the basalt surfaces on Mars), it is more likely that "degassed" and tube-fed basalts would be encountered than the cavernous forms. However, the lavas of the youngest shield volcanoes, such as Olympus Mons and some basaltic plains, are probably more vesicular (especially in near-vent regions) and the likelihood of uncollapsed lava tubes and other subsurface cavities is higher than in the flood basalt regions. Aa and block lava should be expected on the dome volcanoes and composite cones.

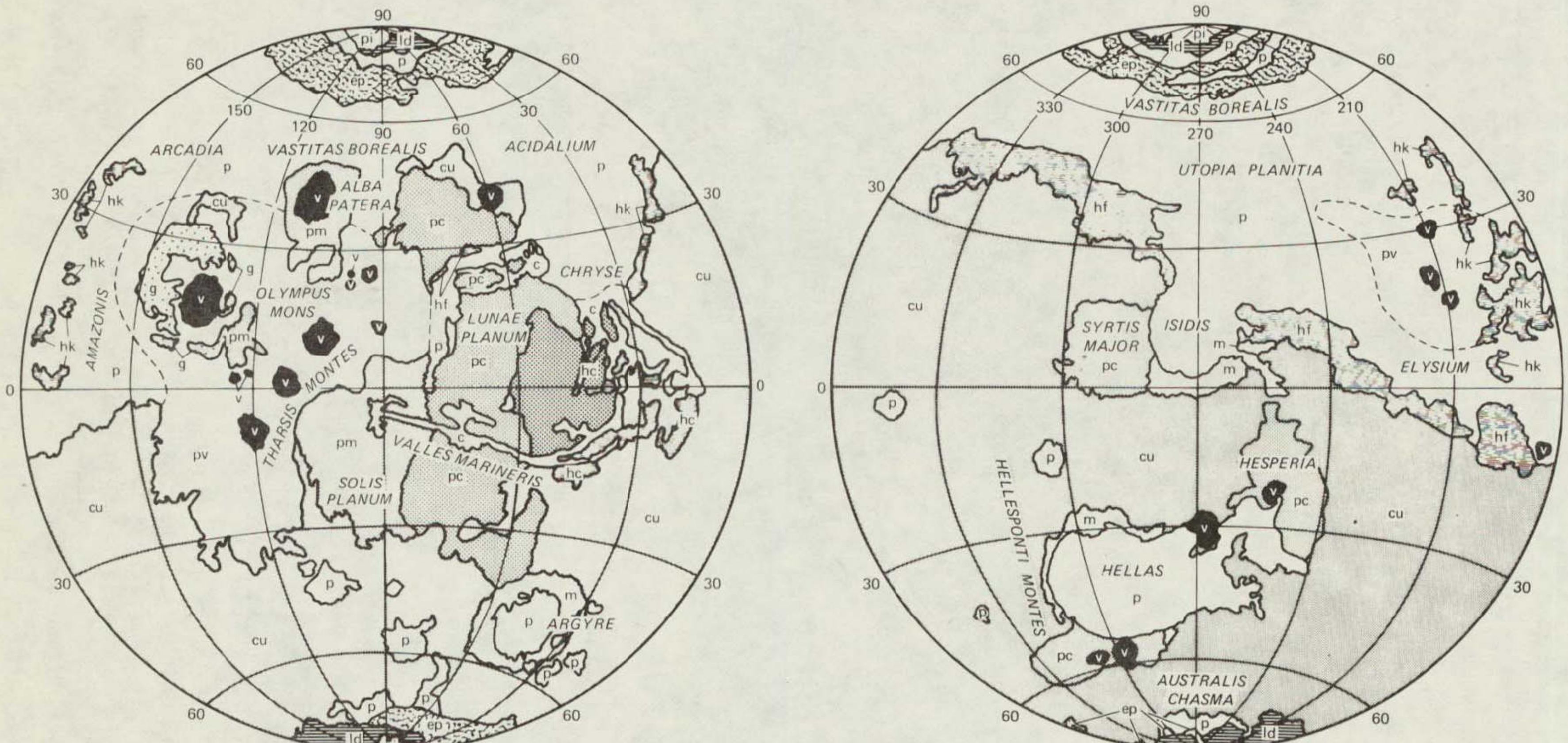

after Mutch et al. in press

Figure 9. Physiographic map of Mars. Volcanic units include constructional features (v) such as shield volcanoes and several types of plains (pv, pm, pc) which appear to be made up of flood basalts and plains basalts.

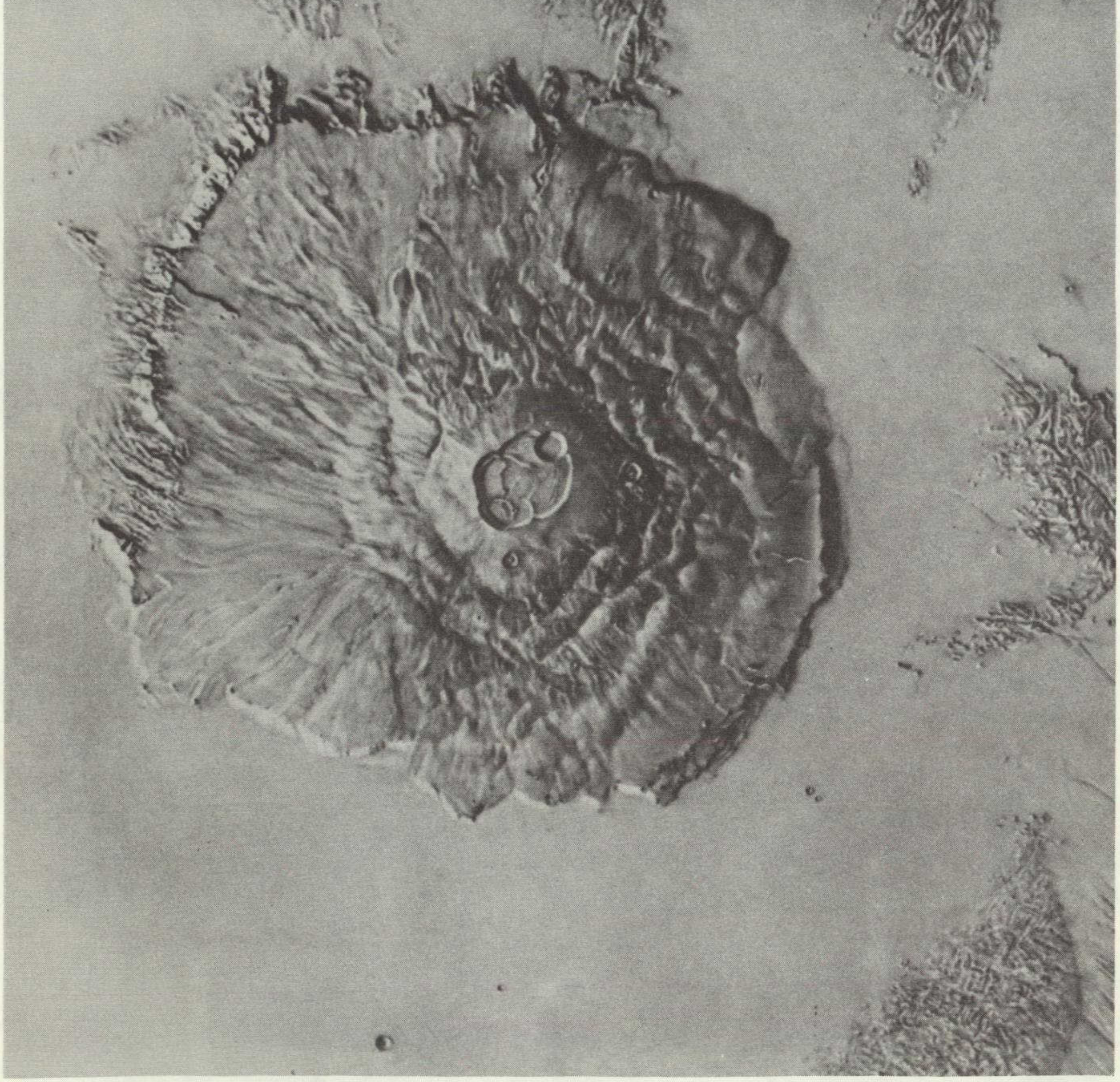

Figure 10(a).- Olympus Mons, the largest volcano in the solar system, is made up of thin basalt lava flows erupted primarily from a central vent (note the summit caldera). Many of the flows are tube-fed. This shield volcano is about 600 km across and, except for its size, is similar in morphology to Mauna Loa, the classic shield volcano in Hawaii. (Airbrush rendition, courtesy of U. S. Geological Survey).

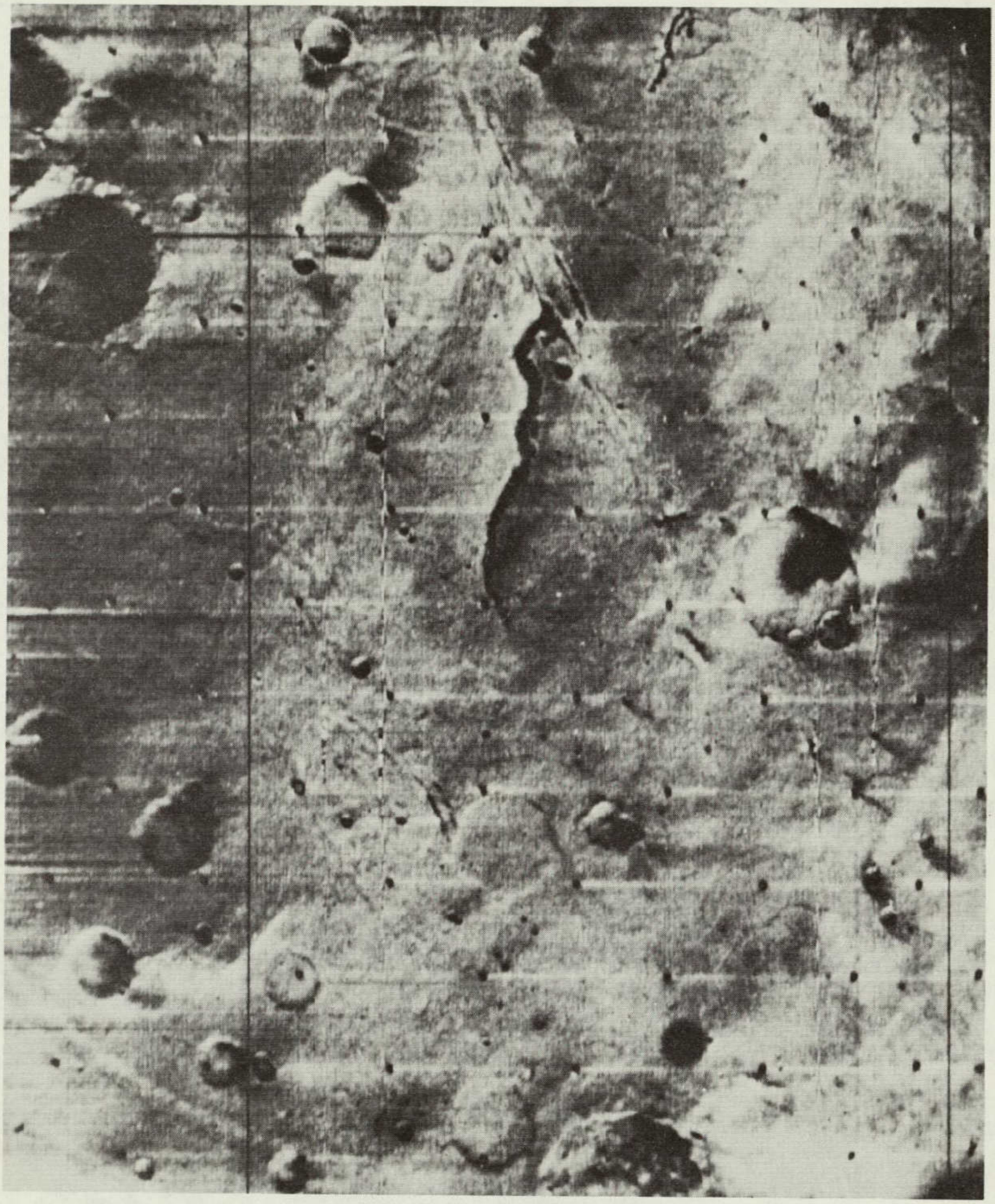

Figure 10(b).- Sinuous channel nearly 100 km long southeast of Valles Marinaris on Mars. Channel appears to originate from an elongate cleft situated on a rift zone. Comparisons with similar features on the Moon and Earth suggest that this feature is a basalt lava flow channel, indicative of basalt plains type activity.

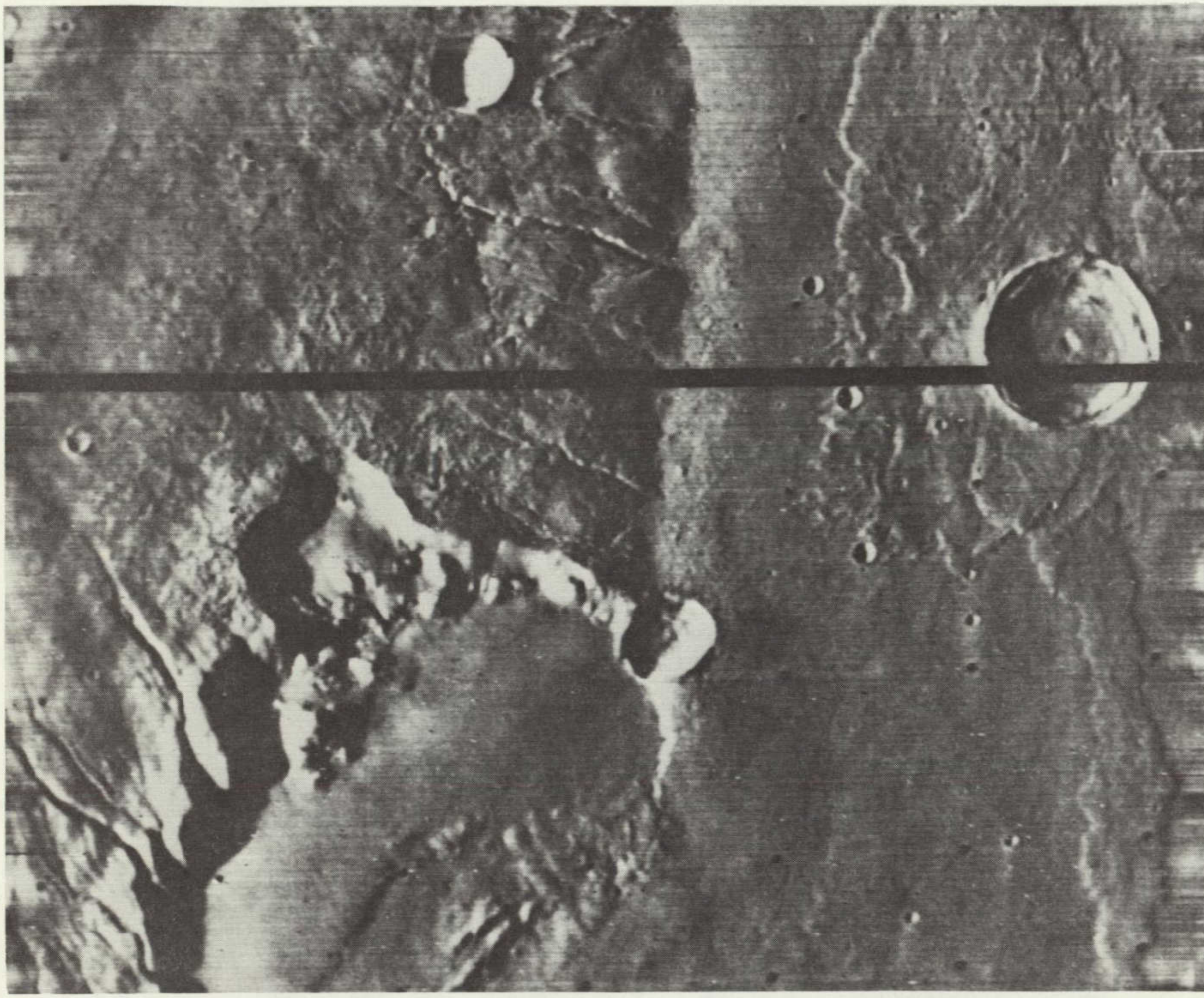

Figure 11.- The Elysium volcanic region on Mars. Area on left side of picture is the flank of one of the constructional volcanoes; area on the right side is made up of younger lava flows. The general morphology of the surface and the distinctive flow lobes resemble mare basalt flows on the Moon and are interpreted to be flood basalts (Mariner 9 frame DAS 13496368).

4.0 AMBOY LAVA FIELD

The Amboy lava field covers about 70 km^2 and consists primarily of "degassed," slightly vesicular pahoehoe lava. The field (figs. 12 and 13) is situated in an alluvial-fill valley between the Bullion Mountains to the southwest and the Bristol Mountains to the northeast; within the valley it lies between Bagdad Dry Lake to the west and Bristol Dry Lake to the east — both playa lakes typical of the Mojave Desert.

Previous geological studies include those of Bassett and Kupfer (1964) who provide a geological reconnaissance of the southeastern Mojave Desert and include a discussion of Amboy Crater, the adjacent alluvial-fill valleys, and the playas, Parker (1963) who studied the volcanism at Amboy Crater, and Hatheway (1971) who included the Amboy lava field as part of an extensive study of basalt "collapse" depressions. A series of open file reports (Watkins, 1965, 1966a,b) of the U. S. Geological Survey include data on Amboy Crater. Studies of eolian processes in the general area are summarized by Smith (1967).

Amboy Crater is a complex cinder cone (fig. 14) about 76 m high and 460 m in diameter which contains an irregular summit crater about 200 m in diameter and 30 m deep. It is in the northeast quadrant of the lava field and has in its wake a dark eolian streak extending more than 3 km downwind. The cinder cone represents the last stages of volcanism on Amboy lava field. It consists primarily of tephra, although the southwestern rim of the cone has been breached by aa flows of limited extent.

Figure 12.- High-altitude (U-2) photograph of the Amboy lava field (north is to the left). (NASA-Ames photograph, courtesy Airborne Sciences Office.)

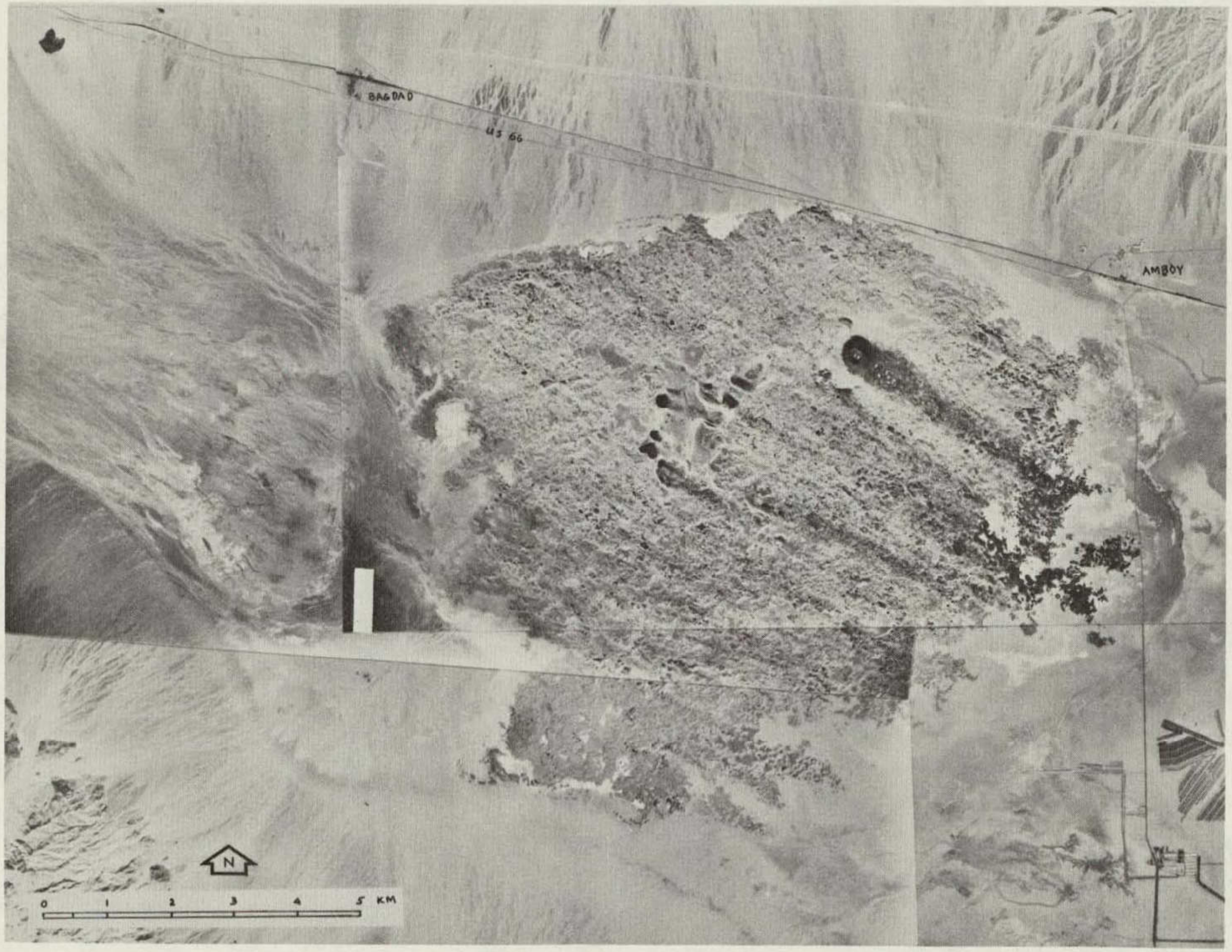

Figure 13.- Mosaic of aerial phptographs of Amboy lava field. Compare with geological map (fig. 15). (U. S. Geological Survey frames VV FS 5737, 5738, 6524, 6525, obtained 1954 and 1955).

Figure 14.- Oblique aerial view of Amboy Crater, a tephra cone representing the most recent volcanic activity on the field. Note the hummocky "degassed" flows in the middle of the pictures flanked by relatively smooth, flat "platform" units. Jeep track at bottom of picture crosses the platform unit selected as test site #1.

4.1 Flow Descriptions

Figure 15 is a geological map after Hatheway (1971), showing the main flow units on the Amboy lava field and the penetrator test sites. Most of the field is composed of undifferentiated flow units made up of relatively dense, degassed pahoehoe lavas that form a hummocky terrain. The surface relief on this unit ranges from 2 to 5 m. The flow is characterized by abundant tumuli (small mounds) and pressure ridges (figs. 16(a),(b)) and, typical of this type of flow, the surface is fractured. Low-lying areas on the flow are filled with eolian (wind-blown) sediments which range from a few centimeters to more than 1 m thick. Thickness of eolian deposits increases toward the southwest part of the field.

Lava tubes are not present in any of the flows, nor are blisters or shelly-type pahoehoe; only a few lava channels are present. Erosion has removed the uppermost glassy and frothy zones of all of the flows and is currently breaking down the vesicular zone, leaving an aggregate of basalt fragments on the surface. Sand blasting is prevalent over the entire flow and wind-faceted pebbles of basalt are common.

The oldest flows occur in the eastern and southeastern part of the field and are characterized (fig. 17) by having numerous "collapse" depressions (circular pits) up to about 10 m in diameter and several meters deep. Although the name would imply that "collapse" depressions formed by the collapse of a crust over fluid lava, recent observations by Holcomb (personal communication) of active lava flows in Hawaii suggest that they may form as a result of inflation of an emplaced, but still plastic, crust by molten lava around a general void in the flow. This mechanism would be more in concert with the general degassed nature of the hummocky pahoehoe. There do not seem to be uncollapsed cavities in any of the flows that make up Amboy lava field. Table 3 gives physical parameters for some of the flows at Amboy.

Two types of flows appear to be appropriate for penetrator tests: *platform units* and *vent lavas* (fig. 15). Platform units are isolated zones of uniform basalt that have relatively flat surfaces. These areas appear to represent stagnant parts of basalt flows that solidified in place with relatively little lateral movement after its emplacement (figs. 14 and 18). Although there are a few collapsed craters on the platform units, they are easily recognized and should not interfere with penetrator drop tests. Detailed examinations (figs. 19(a),(b),(c)) of the flows in cross section (exposed on flow margins and in crater walls) show that the flows are laterally homogeneous. The surfaces of the platform units consist of a layer of fist-sized cobbles of basalt weathered *in situ* from the vesicular zone and wind blown sediments and small basalt fragments several centimeters thick. Test site #1 and test site #3 occur in platform units.

The second type of flow that is a potential test site are the vent lavas (fig. 20), so named because they appear to be situated over the vents for the Amboy lava field. Vent lavas are topographically raised areas about 10 m high that consist of relatively dense pahoehoe. The flows appear to have been "puddled" in relatively stagnant ponds which either drained back down the vent, causing slight crustal collapse on the surface, or which broke out through subsequent flows around the edges of the "puddle." The surfaces are relatively flat and unfractured except around the edges of the puddles. Individual collapse craters (fig. 21) which could represent drain-back in the vents occur in the middle of "puddles." Like the platform areas, the surfaces of the vent lavas have weathered basalt fragments and eolian particles to a depth of several centimeters. Site #2 occurs in one of the vent lava areas (fig. 17).

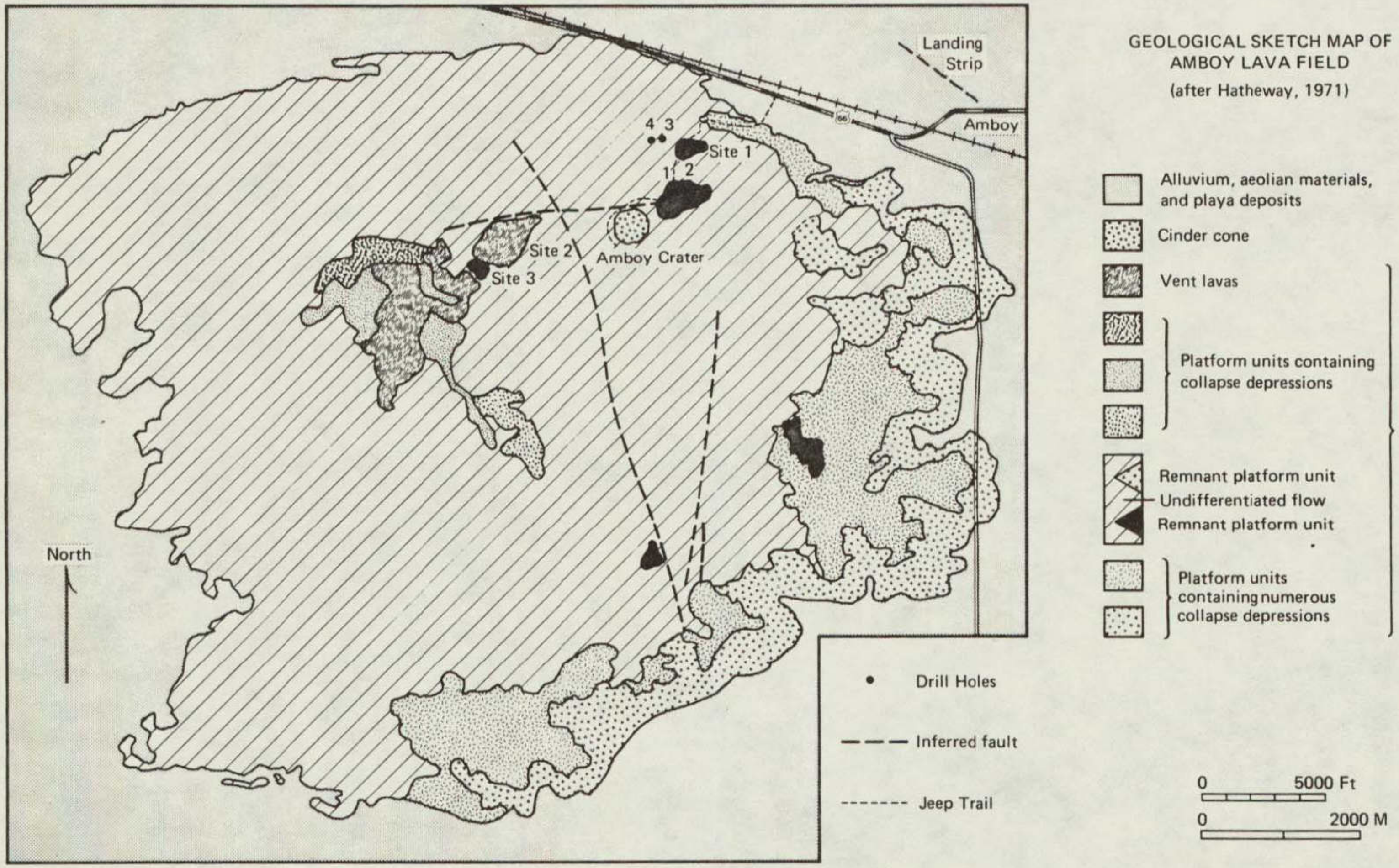

Figure 15.- Geological map of Amboy lava field, showing main lava flows by geomorphic type and their apparent relative age (after Hatheway, 1971).

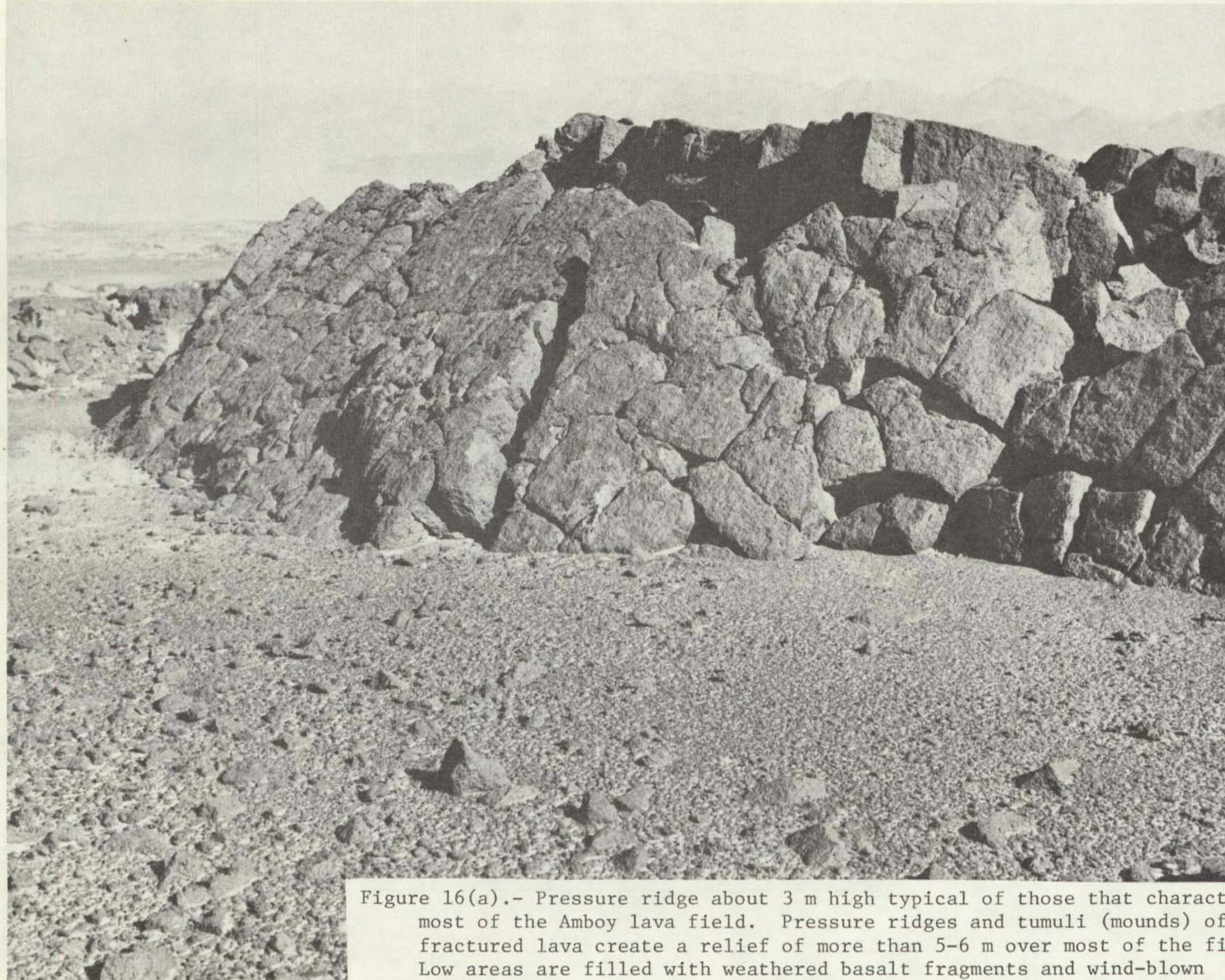

Figure 16(a).- Pressure ridge about 3 m high typical of those that characterize most of the Amboy lava field. Pressure ridges and tumuli (mounds) of fractured lava create a relief of more than 5-6 m over most of the field. Low areas are filled with weathered basalt fragments and wind-blown sediments, as shown here in the foreground.

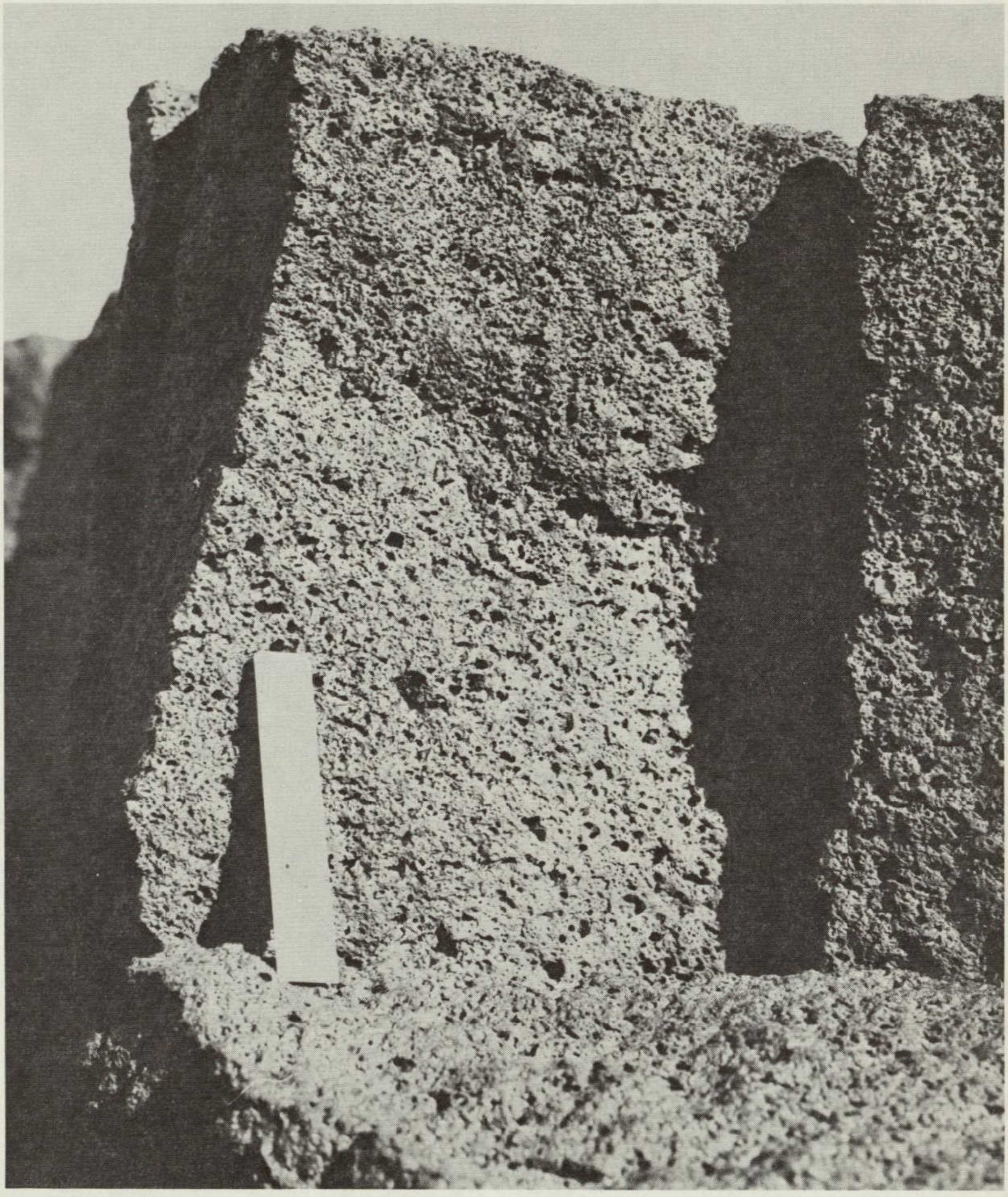

Figure 16(b).- Cross section of the upper vesicular zone, as exposed in the crack of the pressure ridge shown above. Scale is 15 cm long. Vesicularity decreases with depth below the surface.

Figure 17.- Oblique low-altitude aerial photograph of the east end of Amboy lava field, showing the older platform units and circular "collapse" depressions. Flow edges are about 4-5 m high. Low areas are filled with wind-blown sand more than one meter thick in some areas.

TABLE 3.- PHYSICAL PROPERTIES OF AMBOY BASALT

(after Watkins, 1966)

Drill* hole	Porosity (%)	Unconf. compr. strength (kg cm^{-2})	Tensile strength (kg cm^{-2})	Poisson's ratio	Young's modulus (kg $cm^{-2} \times 10^5$)
1	37.7		45.0	0.067	3.17
	10.7		134.4	0.254	6.70
	10.6	118.6		0.254	7.58
2	11.9	70.9		0.180	3.95
	11.8		70.9	0.122	3.23
	4.1	148.0		0.172	3.79
3	23.4	57.4		0.175	2.18
	23.7		23.5	0.208	3.68
	8.1		90.9	0.165	4.66
	10.5	108.8		0.229	3.35
	10.5	116.6		0.233	6.28
	25.3		41.2	0.052	3.10
	11.8		102.5	0.237	5.29
	5.5	268.2		0.208	8.14
4	14.0	75.1		0.220	3.82

*See figure 15 for locations.

Figure 18.- Oblique aerial view westward of test site #1 on the platform unit shown by the arrow (compare with fig. 14). Three collapse depressions occur on the unit. Old Highway 66 is on the right; jeep track crosses the test site.

Figure 19(a).- Typical surface of test site #1, showing small pieces of basalt weathered *in situ* and wind-blown sediments.

Figure 19(b).- Rim of one of the small "collapse" depressions on test site #1.

Figure 19(c).- Cross section of flow at test site #1, as exposed in the depression of figure 19(b), showing typical vesicularity near the surface of the flow.

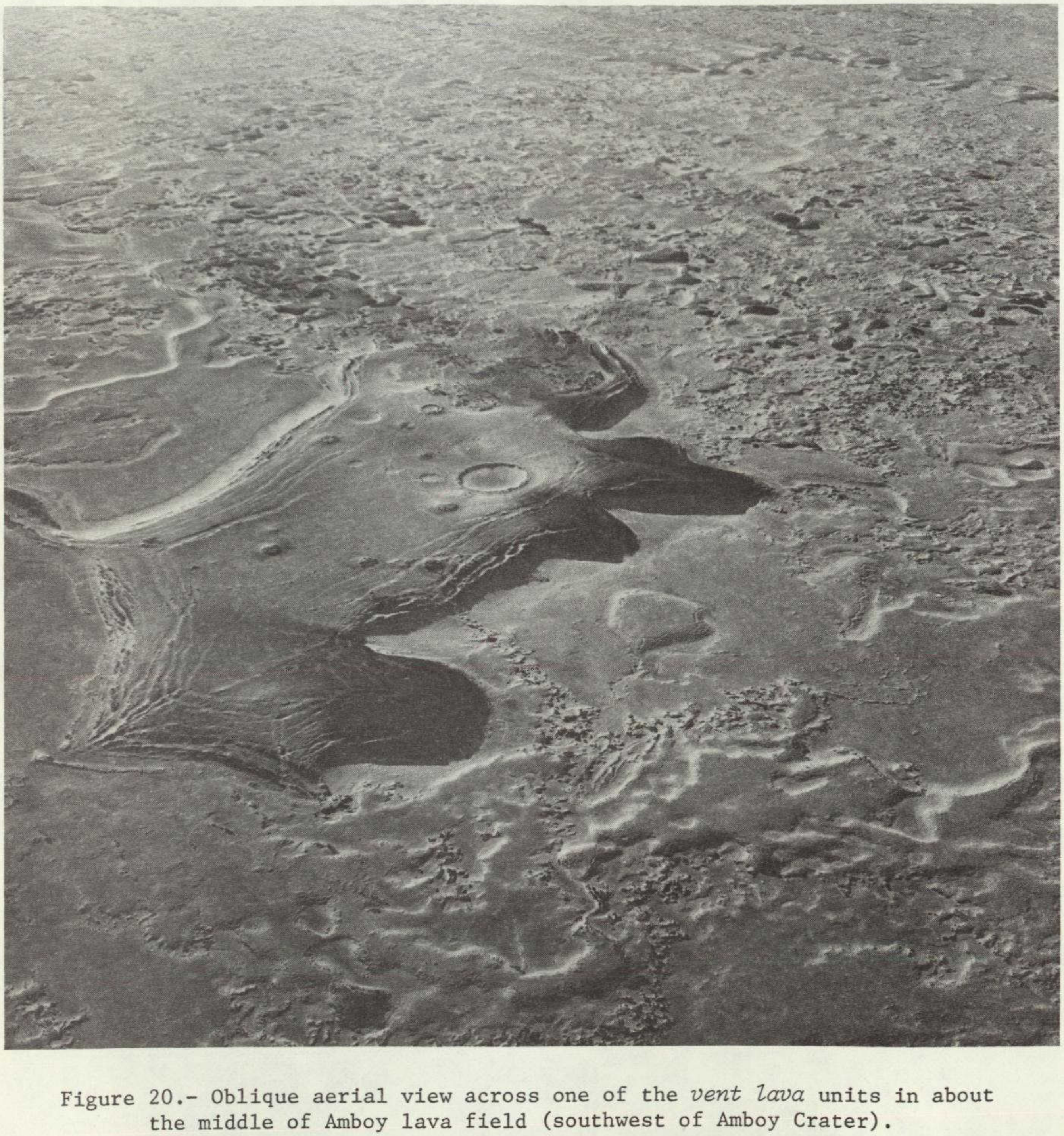

Figure 20.- Oblique aerial view across one of the *vent lava* units in about the middle of Amboy lava field (southwest of Amboy Crater).

Figure 21.- Oblique aerial view across the vent lava unit shown in figure 20, showing a 100-m-diam collapse crater that may have formed by drainback in the vent.

4.2 Test Site Descriptions

Test site #1 — Site #1 is a platform unit about 0.5 mile from the highway (figs. 15 and 18) and is about 460 m long and averages 140 m wide. Several small collapse depressions occur around the margins of the unit (fig. 19). Of the various sites proposed, site #1 is the most readily accessible. High clearance vehicles can be driven onto the flow over a jeep track.

Samples collected from the site show that the basalt is an olivine phyric basalt which is relatively homogeneous with respect to mineral compositions and mineral modes. Olivine phenocrysts and microphenocrysts account for 4-10 vol. percent. In addition, olivine is also present in the groundmass. Electron microprobe analyses of olivine phenocrysts show an average composition of Fo_{81} with cores of Fo_{83} and slight iron enrichment at the margins (Fo_{79}). Microphenocryst crystalliztion overlapped slightly with late-stage phenocryst crystallization as shown by core compositions of Fo_{80} and margins of Fo_{73}. Sparse, but definite groundmass olivine has an average composition of Fo_{71}. Pyroxene (sample 2) is present only as a groundmass phase and shows a range in composition from $Fs_{13}Wo_{49}En_{38}$ to $Fs_{20}Wo_{48}En_{32}$ (fig. 22). Plagioclase laths have an average composition of $An_{60}Ab_{38}Or_{2}$ (labradorite); interstitial glass was not analyzed.

Texture of the basalts are shown in figures 23 and 24. Plagioclase laths are oriented in a pilotaxitic fashion which indicates flow of the partly crystallized rock until final consolidation. The matrix contains little glass, and is composed of interstitial grains of plagioclase, pyroxene, and ilmenite.

Samples of this basalt were collected at 20 different sampling points around the platform unit. Porosity measurements of samples near the surface (0.3 to 0.1 m from the top) have total porosities between 24 and 30% (table 4). Samples taken between 0.5 and 1.0 m from the top show a decrease in porosity and range from 15 to 23%. The very top portion of the unit (upper 10 cm) has a porosity of between 28 and 33%. The calculated average porosity for the upper one meter is $\approx$25%.

An average bulk analysis of three samples collected and described by Parker (1959) from the Amboy lava field is given in table 5. The normative composition of these basalts shows slight nepheline (ne) content and this together with the rather high amounts of Na_2O and K_2O, interstitial alkali glasses, and pyroxene compositions (fig. 22) show that these basalts are alkalic basalts, transitional to high aluminum basalts.

Test site #2 — This site (figs. 16, 25, and 26) occurs in one of the vent lava areas and is 580 m long by 320 m wide. Exposures in a pressure ridge crack (figs. 27(a),(b),(c)) at the northeast end of the site show that the basalt consists of an upper vesicular zone grading into more massive and dense basalt at a depth of about a meter. Although this is the largest of the three sites that was considered, it is also more likely to be laterally variable than either site #1 or site #3. Because the area is a probable vent lava

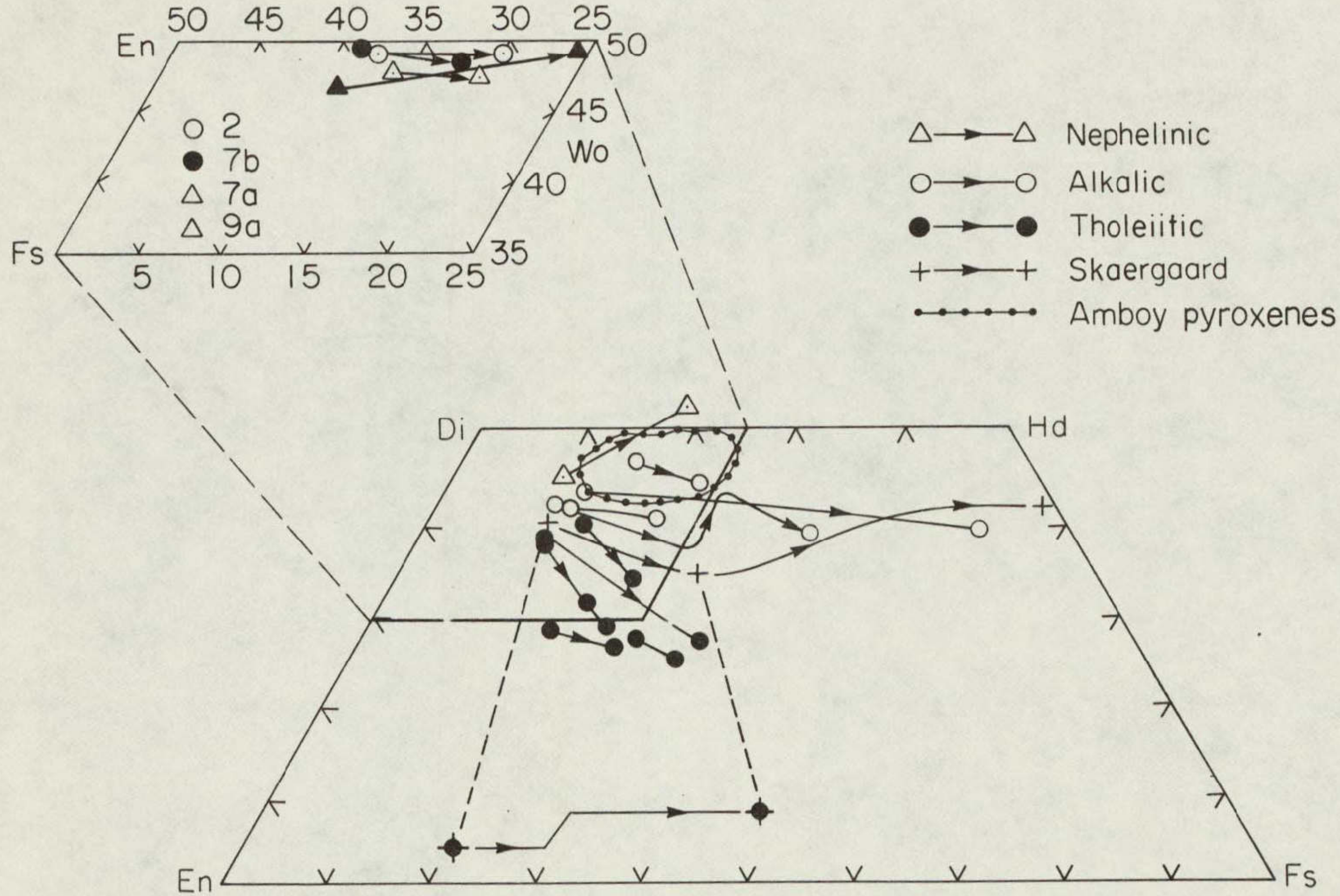

Figure 22.- Pyroxene quadrilateral diagram showing pyroxene differentiation trends of terrestrial basaltic suites, the Skaergaard layered series, and the compositional field of Amboy basalt pyroxenes. The enlarged portion of the diagram shows only Amboy basalt pyroxene compositions and trends.

Figure 23.- Site #1 Amboy lava field, olivine phyric basalt sample 2. Photomicrograph shows olivine microphenocrysts and smaller lath-shaped plagioclase arranged in a pilotaxitic texture (flow orientation). Phenocrysts range up to several millimeters in the hand specimen. Field width = 2.4 mm.

Figure 24.- Olivine phyric basalt, sample 2. Matrix showing a mixture of plagioclase (white), pyroxene (equant and dark), skeletal to equant ilmenite (black) and glass (dark and irregular). Field width = 0.4 mm.

TABLE 4.- POROSITY, BULK DENSITY AND GRAIN DENSITY

MEASUREMENTS OF SITE #1 BASALT SAMPLES

Results of porosity analyses

Analyst: George R. Polkowski
Date: March 17, 1976

Amboy site #1 sample 1a. Top
Total porosity = 26.52%
Bulk density = 2.144 g/cc
Grain density = 2.918 g/cc

Amboy site #1 sample 1b. 50 cm depth
Total porosity = 15.24%
Bulk density = 2.474 g/cc
Grain density = 2.919 g/cc

Amboy site #1 sample 2a. Top
Total porosity = 29.85%
Bulk density = 2.068 g/cc
Grain density = 2.949 g/cc

Amboy site #1 sample 2b. 60 cm depth
Total porosity = 23.38%
Bulk density = 2.277 g/cc
Grain density = 2.972 g/cc

Amboy site #1 sample 4. Representative of top meter
Total porosity = 20.73%
Bulk density = 2.328 g/cc
Grain density = 2.937 g/cc

Amboy site #1 sample 6. Representative of top meter
Total porosity = 21.75%
Bulk density = 2.301 g/cc
Grain density = 2.941 g/cc

See Bunch *et al.* (1976) for measurement methods.

TABLE 5.- AVERAGE CHEMICAL COMPOSITION OF THREE BASALT SAMPLES FROM AMBOY CRATER

(W. H. Herdsman, analyst; Parker (1959))

Original analysis		Normalized to 100% $-H_2O$ and CO_2	CIPW norm	
SiO_2	46.97	47.98		
TiO_2	2.32	2.37	or	9.98
Al_2O_3	16.71	17.07	ab	27.66
Fe_2O_3	4.94	5.05	an	27.23
FeO	5.35	5.47	ne	0.69
MnO	0.19	0.19	di	13.63
MgO	7.24	7.40	ol	11.70
CaO	9.10	9.80	mt	5.28
Na_2O	3.14	3.21	il	3.30
K_2O	1.66	1.69	ap	0.59
H_2O^+	0.65	--		
H_2O^-	0.39	--		
P_2O_5	0.28	0.29		
CO_2	1.06	--		
	100.00	100.00		

Figure 25.- Oblique aerial view eastward of test site #2, showing the vent lava unit (indicated by arrow). Amboy Crater is visible to the upper left. Test site #3 is the platform unit to the right of test site #2 (see fig. 32).

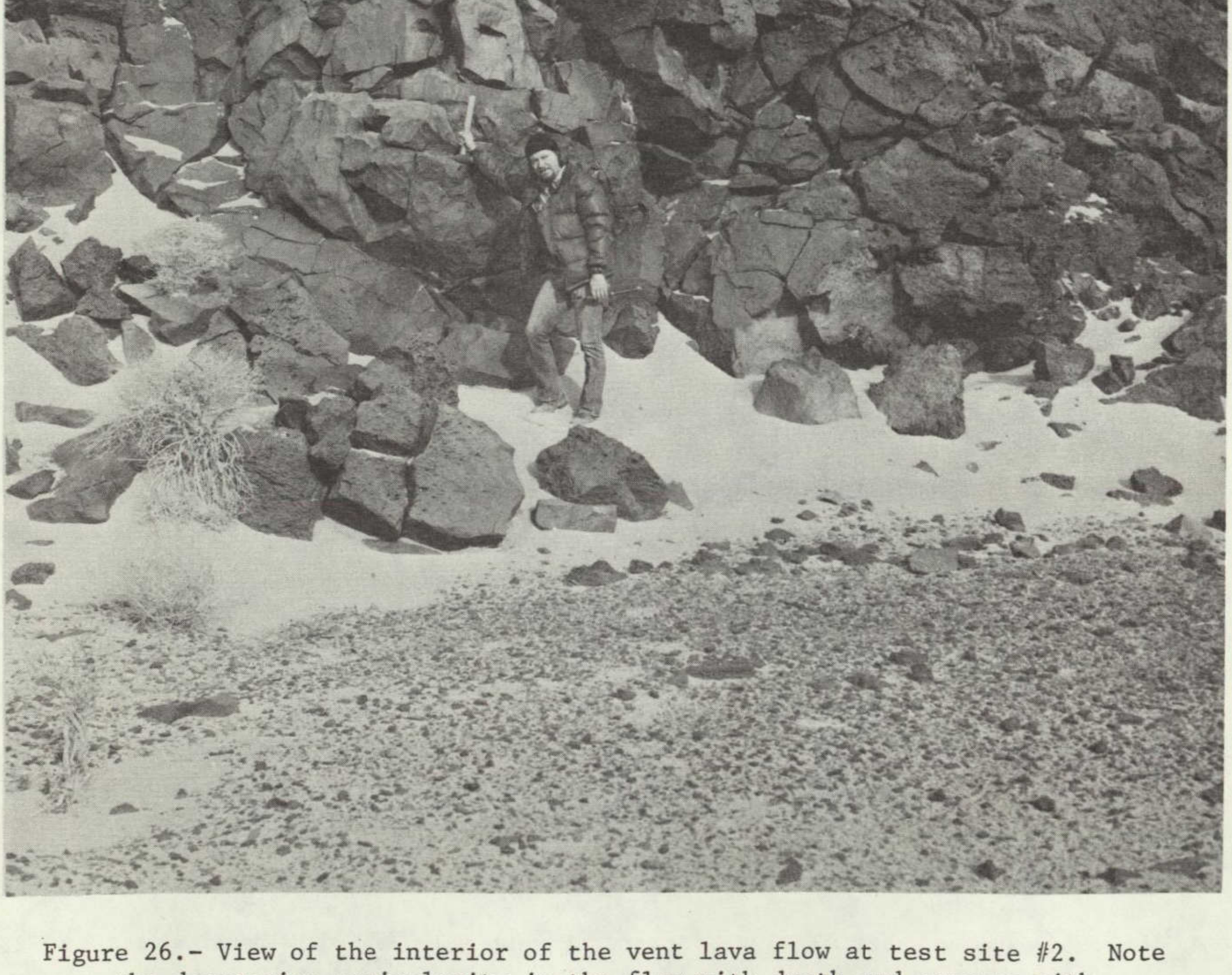

Figure 26.- View of the interior of the vent lava flow at test site #2. Note the decreasing vesicularity in the flow with depth and compare with figure 27.

(a) Upper zone showing vesicular basalt

Figure 27.- Detail of the flow cross section seen in figure 26. The thickness of the vesicular zones is highly variable, with the massive zone within a few centimeters of the surface in some places.

(b) Medium-vesicular zone about 1 m below surface

Figure 27.- Continued.

(c) Massive basalt typical of the flow at a depth of about 2 m.

Figure 27.- Concluded.

flow and because there may have been some circulation within the "puddle," there may be zones within the unit which are relatively degassed in comparison to other units. However, there are not sufficient exposures to determine the degree of variability. An exposure at the southwestern end shows that there are at least two basalt flows involved. The older unit underlying the surface flow is composed of coarse crystalline, dense basalt. The depth of this unit is unknown over the rest of the flow and it may be that the older, dense basalt is close to the surface in some areas.

Samples taken from this flow show that the basalts are similar in texture and mineralogy to basalts of site #1. Sample 7b was collected in the massive, dense zone about 1.5 m from the top of a pressure ridge (just below the vesicular zone). This basalt is an olivine phyric basalt that contains olivine phenocrysts of core composition Fo_{82} and grain margin compositions up to Fo_{77}; microphenocryst core compositions average Fo_{79} and grain margins are as Fe-rich as Fo_{68}. No olivine was observed in the groundmass. Pyroxenes are restricted to the groundmass and range in composition from $Fs_{11}Wo_{49}En_{40}$ to $Fs_{18}Wo_{48}En_{34}$ (fig. 22). Plagioclase laths are labradorite in composition ($An_{63}Ab_{39}Or_{1}$) and interstitial plagioclase is more sodic ($An_{48}Ab_{49}Or_{3}$). Interstitial glass composition is: SiO_2 = 68%; Al_2O_3 = 18.5%; Na_2O = 5.3; K_2O = 7.4%; FeO = 0.60% and CaO = 1.12%; sum = 100.92, which is similar to orthoclase feldspar composition.

The texture is also similar to samples of site #1 (figs. 28 and 29) with pronounced pilotaxitic features, although the matrix is heterogeneous in glass content (fig. 29) with some isolated patches containing considerable glass with very small equant grains of pyroxene and ilmenite in addition to interstitial plagioclase.

Porosity measurements of sample 7b show it to be quite dense with low total porosity (14%). Samples below 7b have even lower densities (<11%).

Sample 7a was collected in the upper vesicular zone about 0.75 m above 7b. Sample 7a shows only vague flow orientation of plagioclase laths (fig. 30) and the olivine has been extensively altered, probably during the degassing process. Less altered olivine phenocrysts have compositions that range from Fo_{94} to Fo_{90} which are extremely Mg-rich. This unusual Mg-rich olivine is probably not original, but became enriched in Mg during autometamorphism of the flow. Figure 31 shows a portion of an altered olivine that contains many specks of iron oxide which probably formed from iron in solid solution in the olivine. X-ray diffraction of the olivine would probably show it to be not of olivine structure but a mixture of altered remnant olivine and secondary minerals (extensive alteration precludes petrographic microscope determination). Groundmass pyroxene is yellow-brown compared with the dark brown color in all other samples studied. The compositional range is from $Fs_{14}Wo_{47}En_{39}$ to $Fs_{19}Wo_{47}En_{34}$. Plagioclase phenocrysts are labradorite ($An_{61}Ab_{33}Or_{1}$); interstitial glass is similar in composition to glass in sample 7b.

The matrix contains pyroxene, ilmenite, plagioclase, Fe-oxides, apatite, and devitrified glass and tends to be granular in texture (fig. 31).

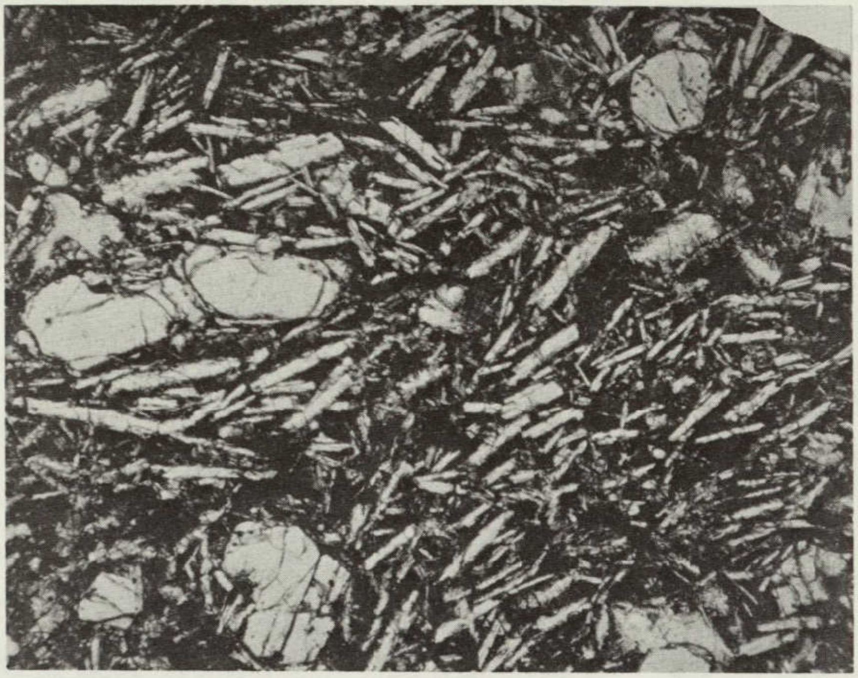

Figure 28.- Site #2 Amboy lava field, olivine phyric basalt sample 7b. Overall characteristics similar to sample 2 (fig. 24). Olivine microphenocrysts are set in a matrix of flow-oriented plagioclase (pilotaxitic texture) and fine-grained augite, plagioclase, and glass. Field width = 2.4 mm. Sample collected from dense, massive zone.

Figure 29.- Olivine phric basalt, sample 7b. Matrix of large amounts of glass, acicular to skeletal ilmenite, plagioclase, pyroxene, and apatite. Field width - 0.4 mm.

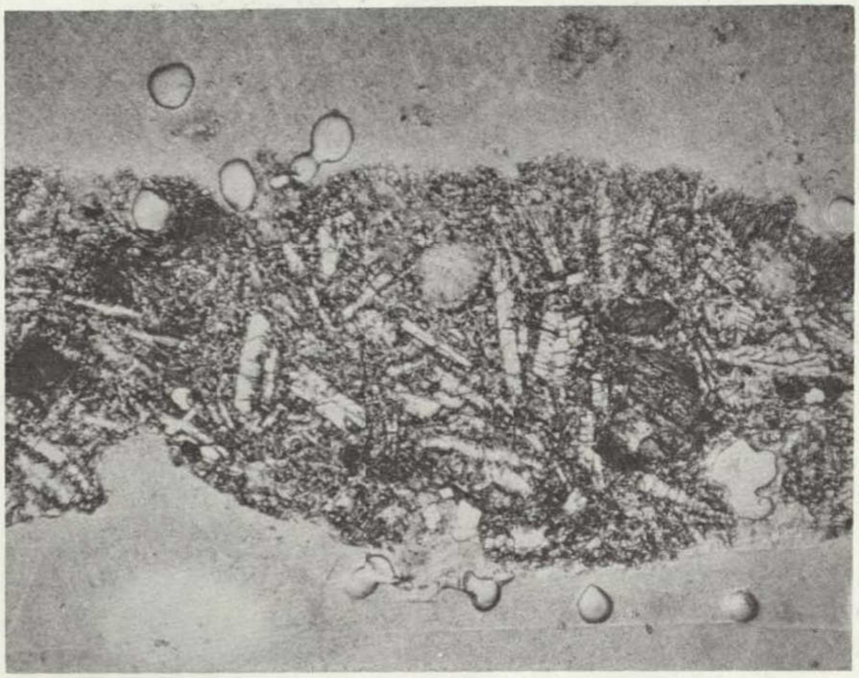

Figure 30.- Site #2, Amboy lava field, olivine phyric basalt sample 7a. Handsample shows few olivine phenocrysts. Photomicrograph shows altered olivine microphenocrysts and fresh plagioclase laths that have a vague flow orientation. Field width = 2.4 mm. Sample collected in the vesicular zone above 7b.

Figure 31.- Olivine phyric basalt, sample 7a. Granular matrix of yellow augite (grey), glass (grey), plagioclase (white) and equant ilmenite and Fe-oxides (black). Large grain to the left is altered olivine with high concentration of Fe-oxides around the margins and within the interior. Field width = 0.4 mm.

Test site #3 — This test site occurs southwest of the puddled vent lavas of test site #2 (fig. 16). It is an area about 240 m long and 110 m wide, situated in a low-lying area between the vent lavas (fig. 25). Like test site #3, it appears to be a platform unit that has a fairly uniform surface and homogeneous texture across the entire unit (figs. 32 and 33). There is, however, one collapse crater at the northwest end of the platform which could interfere with a penetrator test drop.

Samples from this area show that the basalts are different than the other sites in having both olivine and plagioclase phenocrysts (figs. 34 and 35). These basalts are referred to as simply phyric basalts. Sample 9a contains olivine phenocrysts of Fo_{81} and grain margins of Fo_{72}. Microphenocrysts have a limited compositional range of Fo_{73} to Fo_{71}. Pyroxene is found only in the groundmass and has a rather extensive compositional range of between $Fs_{11}Wo_{46}En_{43}$ and $Fs_{24}Wo_{49}En_{27}$ (fig. 22). Plagioclase phenocrysts are labradorite ($An_{60}Ab_{38}Or_2$) and are relatively homogeneous; plagioclase laths are $An_{57}Ab_{41}Or_2$. Interstitial glass composition is also very similar to that in samples 7a and 7b. The matrix of sample 9a contains abundant skeletal crystals of ilmenite, Fe-oxides and sulfides, equant brown pyroxene interstitial plagioclase and glass.

Porosity measurements range from 28% near the surface to 16% at a depth of 1.0 m.

Test sites #2 and #3 are accessible only by high clearance four-wheel drive vehicles driven in from the highway over a jeep trail that goes past the cinder cone. The jeep trail beyond the cinder cone is poorly defined.

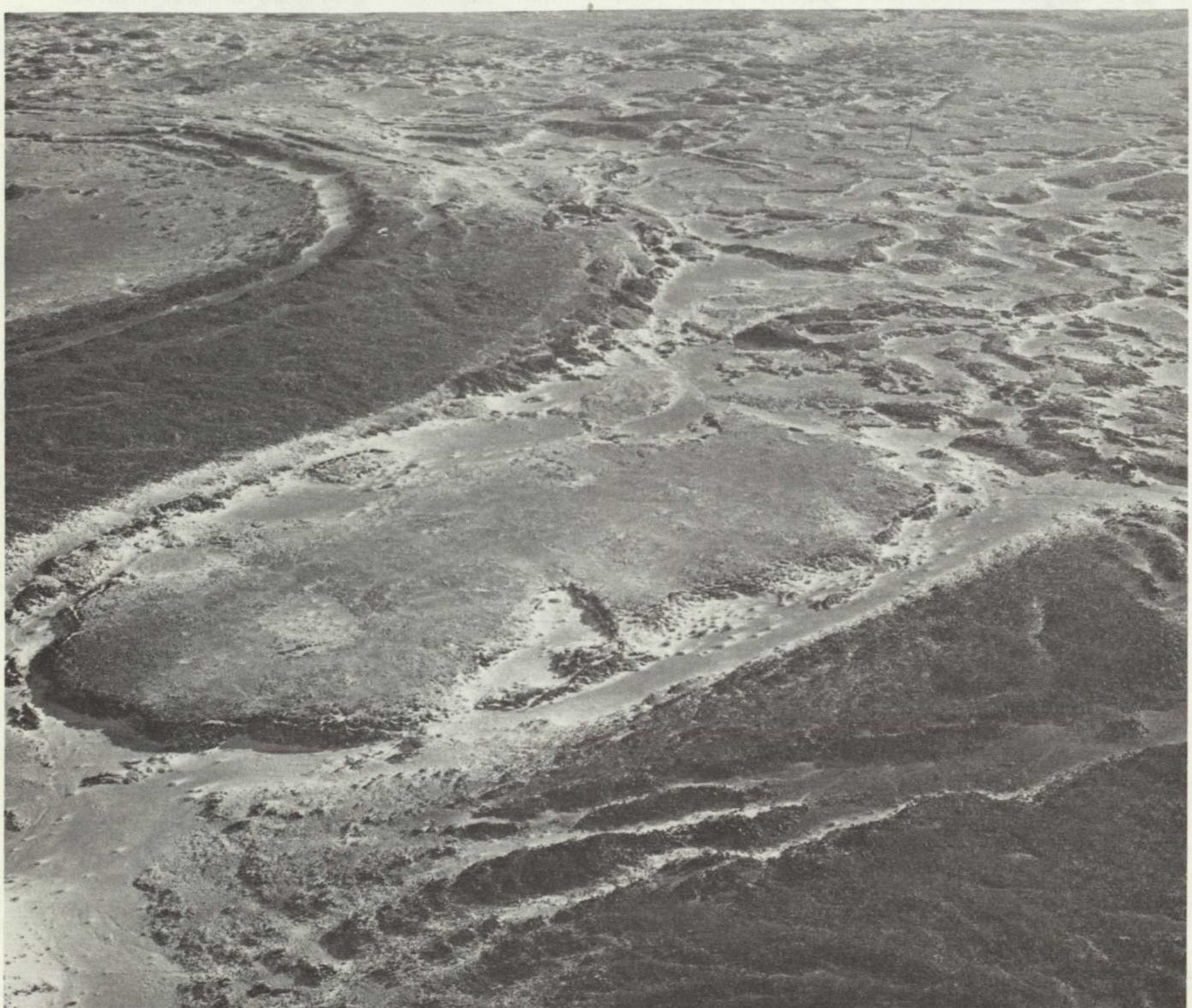

Figure 32.- Oblique low altitude photograph across the platform unit that comprises test site #3.

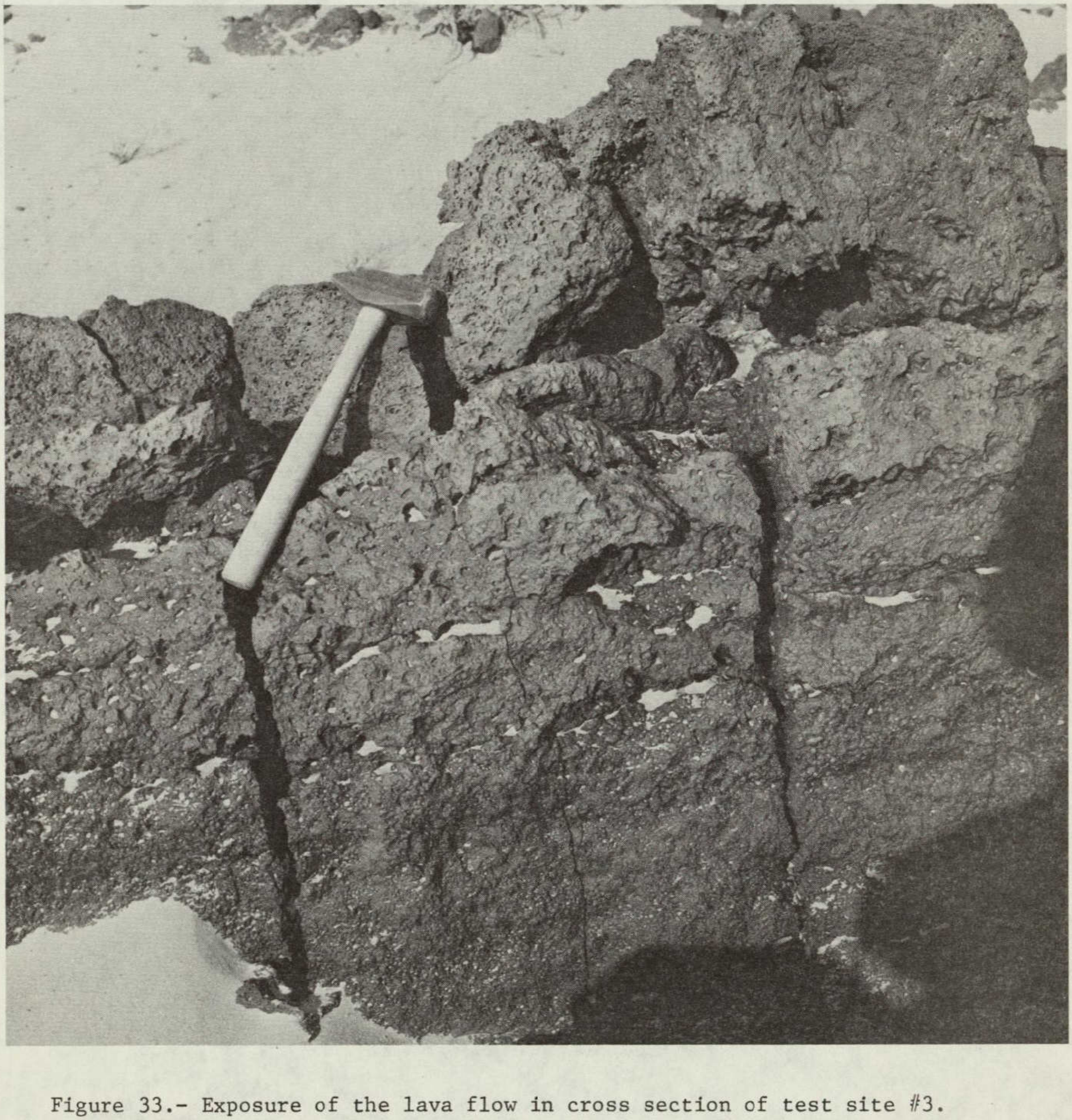

Figure 33.- Exposure of the lava flow in cross section of test site #3.
Head of hammer is at the flow surface.

Figure 34.- Site #3, Amboy lava field, phyric basalt sample 9. Phenocrysts of both olivine and plagioclase reach 2-4 mm in maximum dimension. Flow orientation is not well developed. Field width = 2.4 mm.

Figure 35.- Phyric basalt, sample 9. Dark matrix composed of large amounts of dendritic ilmenite and Fe-oxides, glass, pyroxene and plagioclase. Field width = 0.4 mm.

5.0 SUMMARY

The Amboy lava field consists of several pahoehoe flow units, mostly of the "degassed" variety, that form a hummocky terrain of 4-5 m relief. Some of the units, notably "platform" and "vent" lavas form flat, homogeneous surfaces several hundred meters square. Erosion has removed the glassy and frothy zones typical of fresh pahoehoe from all of the flows at Amboy, leaving the vesicular zone and massive zones. Vesicularity ranges from more than 40% near the surface to less than 10% in the massive zone; the rate of change in vesicularity with depth is variable from one area to another. Basalts from the three sites range from olivine phyric to olivine-plagioclase phyric with variable amounts of matrix glass. Pyroxene compositions and differentiation trends are more consistent with alkalic basalts than with tholeiites. Most basalts show flow orientation of plagioclase laths. Average porosities for the three sites are between 23 and 26% for the top one meter.

Considering the types of basaltic terrains on Mars and the probable degree of weathering and variable depths of impact-generated regolith, the target areas selected at Amboy are probably representative of the majority of the basalt flow surface on Mars to a first-order approximation. On the other hand, the freshest pahoehoe flows associated with some of the shield volcanoes and vent areas of plains basalt on Mars may be more vesicular than the Amboy basalts and have shelly pahoehoe and uncollapsed cavities such as lava tubes and blisters.

REFERENCES

Bassett, A. M.; and Kupfer, D. H.: A Geologic Reconnaissance in the Southeastern Mojave Desert. Special Rep. 83, Calif. Div. Mines and Geology, 1964.

Briggs, G. A.: Mars Polar Orbiter/Penetrator Study Report. Rep. 760-129B, Jet Prop. Lab., 1975.

Bunch, T. E.; Quaide, W. L.; and Polkowski, G.: Initial Basalt Target Site Selection Evaluation for the Mars Penetrator Drop Test. NASA TM X-73,111, 1976.

Carr, M. H.: Volcanism on Mars. J. Geophys. Res., vol. 78, 1973, pp. 4049-4062.

Carr, M. H.: Tectonism and Volcanism of the Tharsis Region of Mars. J. Geophys. Res., vol. 79, 1974, pp. 3943-3949.

Cutts, J. A. J.: Evaluation of the Feasibility of Experiments for a Mariner Class Mars Polar Orbiter Mission with Multiple Penetrator Surface Probes. Internal report for Space Science Division, Jet Prop. Lab., 1975.

Elston, W. E.; Aubele, J. C.; Crumpler, L. S.; and Eppler, D. B.: Influence of Tectonic Setting, Composition, and Erosion on Basaltic Landforms: New Mexico and Mars. Reports of Accomplishments of Planetology Programs, 1975-1976, NASA TM X-3364, 1976, pp. 129-132.

Greeley, R.: Modes of Emplacement of Basaltic Lavas and an Analysis of Mare Volcanism in the Orientale Basin. Presented at Proc. Seventh Lunar Sci. Conf., 1976.

Greeley, R.; and King, J. S.: Geologic Field Guide to the Quarternary Volcanics of the South-Central Snake River Plain, Idaho. Pamphlet 160, Idaho Bureau of Mines and Geol., 1975.

Greeley, R.; Wilbur, C.; and Storm, D.: The Role of Lava Tubes and Channels in the Construction of Mauna Loa Shield Volcano (in preparation).

Hatheway, A. W.: Lava Tubes and Collapse Depressions. Ph.D. Thesis, Univ. of Arizona, 1971 (unpublished).

Macdonald, G. A.: Volcanoes. Prentice Hall, Inc., 1972.

Mutch, T. A.: A Geologic Atlas of Mars. Princeton Univ. Press (in press).

Parker, R. B.: Recent Volcanism at Amboy Crater, San Bernardino County, California. Special Rep. 76, Calif. Div. Mines and Geology, 1963.

Quaide, W. L.: Mars Science Missions in the Post-Viking Era: Possible Contributions of Pioneer Type Missions. Internal Rep. of Space Sciences Division, NASA Ames Research Center, 1974.

Smith, H. T. U.: Past Versus Present Wind Action in the Mojave Desert Region, California. Rep. 67-0683, Air Force Cambridge Research Lab., 1967.

Swanson, D. A.: Pahoehoe Flows From the 1969-1971 Mauna Ulu Eruption, Kilauea Volcano, Hawaii. Geol. Soc. Amer. Bull., vol. 84, 1973, pp. 615-626.

Watkins, J. S., ed.: Investigation of *In Situ* Physical Properties of Surface and Subsurface Site Materials by Engineering Geophysical Techniques. U. S. Geol. Survey Project Rep. to NASA for fiscal year 1965, 1965.

Watkins, J. S., ed.: Investigation of *In Situ* Physical Properties of Surface and Subsurface Site Materials by Engineering Geophysical Techniques. U. S. Geol. Survey Quarterly Rep., 1 Oct 1965 to 31 Dec 1965, 1966a.

Watkins, J. S., ed.: Investigation of *In Situ* Physical Properties of Surface and Subsurface Site Materials by Engineering Geophysical Techniques. U. S. Geol. Project Rep. to NASA for Fiscal Year 1966, 1966b.

Wentworth, C. K.; and Macdonald, G. A.: Structures and Forms of Basaltic Rocks in Hawaii. Bull. 994, U. S. Geol. Survey, 1953.